Final Report

Axial Flux Permanent Magnet Bi-directional Rotary Actuator

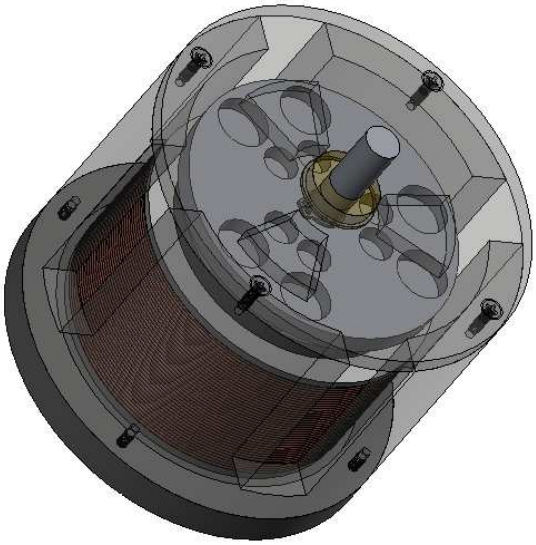

Sung Bae
Robert Hooge
Chris Imparato
Jose Jaramillo

Sponsored by:
Sandia National Laboratories
Sponsor:
Gilbert Benavides

April 1, 2008

Table of Contents

1 Introduction 1
2 Problem Definition 1
3 Background 2
4 Design and Analysis 3
4.1 Concept Generation and Selection 3
4.1.1 Design 1 4
4.1.2 Design 2 5
4.1.3 Design 3 6
4.1.4 Final Design 7
4.2 2D Modeling and Analysis 8
4.2.1 Maxwell 2-D Model 8
4.2.2 Maxwell 2-D Analysis 9
4.3 3D Modeling and Analysis 10
4.3.1 Maxwell 3-D Model 10
4.3.2 Maxwell 3-D Analysis 11
4.3.3 Thermal analysis on E-Physics 13
4.3.4 Optimization 14
4.4 Prototype 16
4.5 Materials Selection 17
5 Fabrication and Assembly 18
5.1 Fabrication 18
5.1.1 Rotor and Shaft 18
5.1.2 Stators 19
5.1.3 Base Plate and Housing 20
5.1.4 Spool and Coil Core 20
5.1.5 Winding Fixture Fabrication 21
5.1.6 Coil Fabrication 21
6 Assembly 23
6.1 Assembly 23
6.1.1 Rotor Assembly 23
6.1.2 Full assembly 24
7 Testing 28

7.1 Testing 28
7.1.1 Thermal testing 28
7.1.2 Torque Testing 29
8 Conclusions and Recommendations 31
8.1 Conclusions 31
8.2 Recommendations 31
8.3 Acknowledgements 32

Appendices

Appendix A: Calculations 33
Appendix B: Graphs 38
Appendix C: Materials 42
Appendix D: Diagrams 44
Appendix E: Solidworks Drawings 47
Appendix F: Reference Papers 64

Table of Figures

Figure 4.1 - Operational Schematic 3
Figure 4.2 - Original Design 4
Figure 4.3 - Basis for actuator design 5
Figure 4.4 - Operation of two stator actuator 6
Figure 4.5 - Operation of single coil surrounding rotor 7
Figure 4.6 - Final design cross-sectional view 8
Figure 4.7 - 2D model of rotary actuator 9
Figure 4.8 - Magnetic field magnitude plotted on surface 10
Figure 4.9 - Magnetic flux lines plotted on surface 10
Figure 4.10 - Cross section of 3D model 11
Figure 4.11 - Outer housing magnetic flux plotted on surface 12
Figure 4.12 - Inner parts magnetic flux plotted on surface 12
Figure 4.13 - Magnetic field lines in actuator 13
Figure 4.14 - Temperature distribution on surface of actuator 14
Figure 4.15 - Torque vs. magnet angle 15
Figure 4.16 - Actuator model assembly 16
Figure 4.17 - Actuator model exploded view 16
Figure 4.18 - Dimensions of NdFeB magnets in system 17
Figure 5.1 – Rotor and Shaft 19
Figure 5.2 - Lower and Upper Stators 19
Figure 5.3 - Base plate and Housing 20
Figure 5.4 - Spool and Coil core 21
Figure 5.5 - Winding fixture parts 21
Figure 5.6 - Spool on winding lathe (left) and Completed Coil (right) 22
Figure 6.1 - Completed rotor sub-assembly 23
Figure 6.2 - Fabricated parts 24
Figure 6.3 - Base plate and Coil core 25
Figure 6.4 - Coil added 25
Figure 6.5 - Lower stator added 26
Figure 6.6 - Outer Housing attached 26
Figure 6.7 - Rotor assembly added 27
Figure 6.8 - Fully assembled actuator 27
Figure 7.1 - Testing setup 28
Figure 7.2 - Thermal Testing after 2 min. 47.4°C (left) and 5 min. 53.2°C (right) 29
Figure 7.3 - Torque test 30

Executive Summary

The Compact Bi-directional Rotary Actuator project is sponsor by Sandia National Laboratories. This actuator project was based on Micro-Electro-Mechanical Systems (MEMS) technology. However, the actuator prototype design and construction would be scale up due to lack of knowledge and access to the technology and for budget constraints. The model actuator is going to have 2 inches. Soon after the actuator prototype is conclude and approved, the Sandia Labs would scale it down to their specific needs. The desire application of this step motor design is to be part of a locking mechanism for an unspecified weapon system.

The step motor design had almost no room to play with. Our sponsor representative, Gilbert Benavides from Sandia National Laboratories, had specific needs for the motor. Such specifications were the used of one coil, a pancake style design, one set of outer poles, one set of inner poles, and a compact and easy to assemble housing, and a torque of 0.3 Nm. Other factors were left for the team and advisors to decide. For instance, dimensions, materials, air gaps, inside arrangements, and housing. Even though specifications are made, designing a mechanism involving such requirements it is not an easy task to reach because so many needs produce many limitations.

To reach the goals require by our sponsor, we had to utilize a computer simulation program call Maxwell 2D and 3D. The advisors for the project, Dr. Philippe Masson and Dr. Ongi Englander, were very helpful in guiding the team through these programs. The Maxwell software was used to determine how much current the coil needs, size of air gaps, position of magnets, and other specifications to achieve the necessary torque. Using Maxwell not only estimated answers, but it saved time, labor, funds, and defiantly takes the project in the right path. The latest model developed in Maxwell output the following results; using 1500 Amps turns torque result in 0.42141 Nm, while temperature reached 71.4 °C. Furthermore, the Bi-directional Rotary Actuator project is currently a computer and paper design only, which meets expectations for the time being. The project has enough data to proceeds with the fabrication and testing of a tangible mechanism.

1 Introduction

The Bi-directional Rotary Actuator assigned by the Sandia National Laboratories for the senior design project is related to MEMS technology. This field is responsible for fabrication of electro-mechanical systems on a microscopic scale using integrated circuit process sequences. MEMS' more commonly fabricated mechanisms are sensors and actuators. A pancake style actuator with one coil and a compact design is what the project final deliverable was. An actuator or step motor is a mechanism that transforms electrical power into mechanical force. However, these types of motors are not in constant motion and do not need a brake system to stop them. These motors move in steps how their names, highlights, and those distances are set according to each specific need. Gilbert Benavides from Sandia Labs had a need assessment for the motor to rotate in steps between 20-30 degrees.

For the past two semesters, our team has been working with one general design, which has had small modifications specifically in dimensions and material selection. Due to so many needs required by our sponsor, the mechanism's esthetic cannot change much. After manipulating the idea on simulation software (Maxwell), our team has found that the required torque of 0.3 N-m is feasible. In addition, calculation results explain that the actuator in operation would produce more than 70 degrees Celsius. This temperature is achieved when the device is at steady state and would require a heat removal system. Given the device will not be on long enough to reach steady state a heat removal system was not designed.

2 Problem Definition

The project was to design and fabricate a bi-directional rotary actuator for Sandia National Laboratories. The concept modifies an original design that has two single-directional solenoids and reduces it to one bi-directional solenoid. The goal is to duplicate or improve the performance by using only one coil. This single coil will reduce the weight as well as the size of the overall device. If successful, the design will be scaled down to nano or micro size and used as a safety device for weapons.

3 Background

In order to understand how a bi-directional rotary actuator works it is necessary to understand the principles of magnetism and electromagnetic motors. Magnetism is one of the peculiar physical characteristics, which is caused by acts of the attractive or repulsive forces within a magnetic field. Magnetic fields can be seen where magnetic forces of magnetic dipoles are detected. It also occurs by electrical currents through wires because those electrical currents affect the others, which is called electromagnetism. Specifically, the motion of electrons produces magnetic field because every electron has a magnetic attribute. Magnetic force is calculated by cross product of electric charge, velocity of charged element, and magnetic field; Fleming's left hand rule is applied to the force. In the rule, thumb, index finger, and middle finger indicate the direction of motion, field, and current respectively. The direction of the force is perpendicular to the magnetic field. Usually electromagnets are used for electromagnetism, which consists of a magnetic substance and coils wrapping around it. Iron, steel can be used as magnetic materials because magnets can attract those metals. When electric currents pass though the coils, the metal core is magnetized. The magnetized metal acts like a magnet, but the magnetic effect disappears when the current is not applied. The power of magnetic effect depends on the number of coils and the quantity of electrical current. By contrast, permanent magnets have magnetic attributes produced by the natural movement of electrons. Mainly mixtures of iron, cobalt, and nickel are used for permanent magnets.

In many fields, electromagnetism is used. An electric motor is one of the most important uses of magnets. It can switch electrical energy to mechanical energy. There are two types of electric motors: rotary and linear motors. The difference between two types of motors is the direction of movement based on how to assemble them. In addition, an electrical motor can be classified by DC type and AC type. Among rotational actuators, a stepping motor has several advantages over other types of motors. It is able to position accurately because the number of poles on a stator and permanent magnets on a rotor can control the degree per step of the rotary actuator. Moreover, the rotary actuator can produce the highest torque at low speed. When currents are applied to a coil, poles on the stator are magnetized axially and magnetic field is formed. As magnetized poles act as electromagnets, they are in alignment with the opposite poles of the permanent magnet on the rotor by attracting them and repelling the same poles of the

permanent magnet on the rotor. This procedure makes the rotor rotate in one direction with a specific angle. By the opposite direction of the current applied to the coil, the rotor will rotate in the other direction.

4 Design and Analysis

4.1 Concept Generation and Selection

Our design is based on the principles of an axial flux electric motor. When a current-carrying conductor is placed in a magnetic field, it is subjected to electromagnetic force or Lorentz force. This force is fundamentally important because it is the foundation of the motor operation. The magnitude of this force depends on orientation of the conductors with respect to the magnetic field. The force is at its maximum when the conductor is perpendicular to the magnetic field and becomes zero when it is parallel.

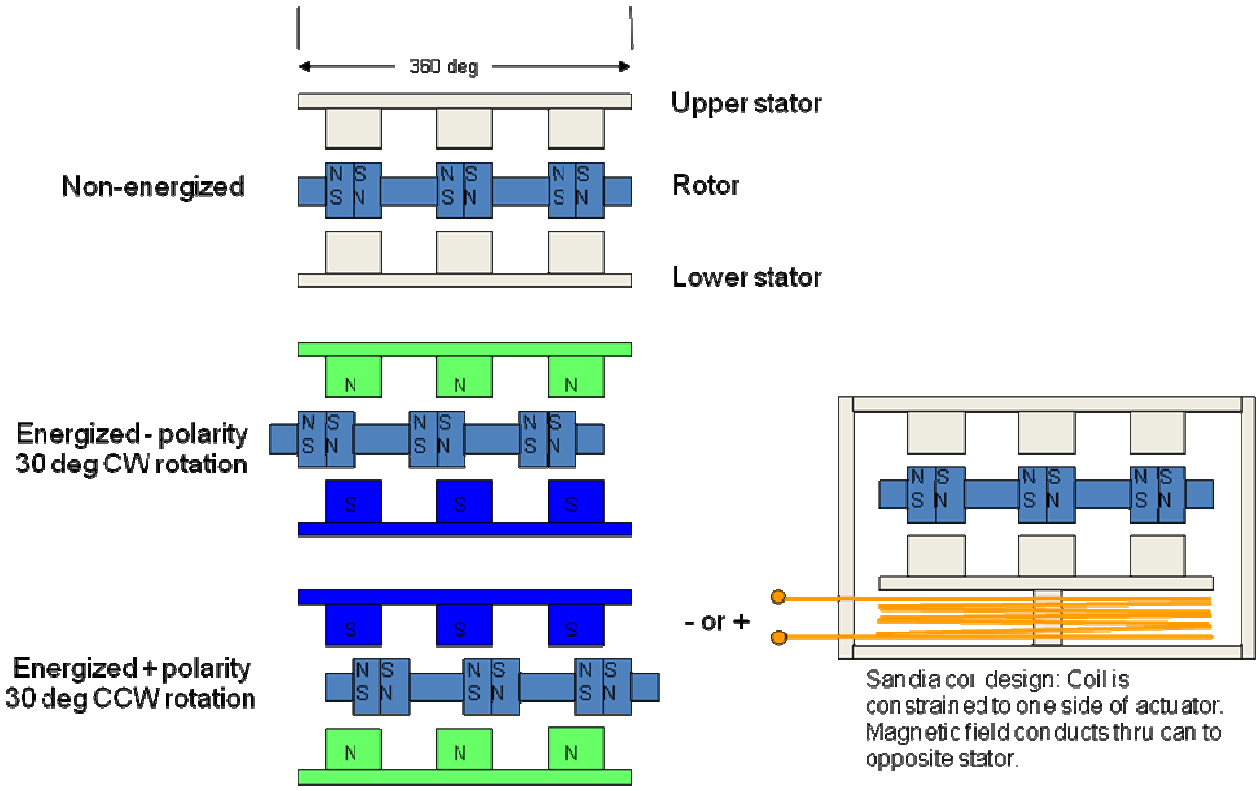

Figure 4.1 - Operational Schematic

Figure 4.1 above illustrates the operation of the designs. When the actuator is not energized the rotor is in a neutral position. Depending on what polarity the stators are magnetized in, the rotor will move to a new position**.**

4.1.1 Design 1

This design calls for the use of one coil to operate the rotor. The single coil allows the actuator to be very small and lightweight. The design is considered a pancake style design because the coil will be directly above the rotor not surrounding the rotor. The direction of the rotor is controlled by the direction of the current flowing through the coil. For example if the current flows left to right, then the rotor rotates clockwise and vice versa. When the coil has no current flowing through it, then the rotor will return to its neutral position. This actuator will rotate both clockwise and counterclockwise approximately 22.5º. For an actuator of a certain size, it takes advantage of the rotors maximum moment arm. This means that the radius of the rotor is its maximum given the radius of the entire actuator. This design contains a mounting plate, an outer housing, an inner pole, an outer pole, a coil, and a permanent magnet rotor.

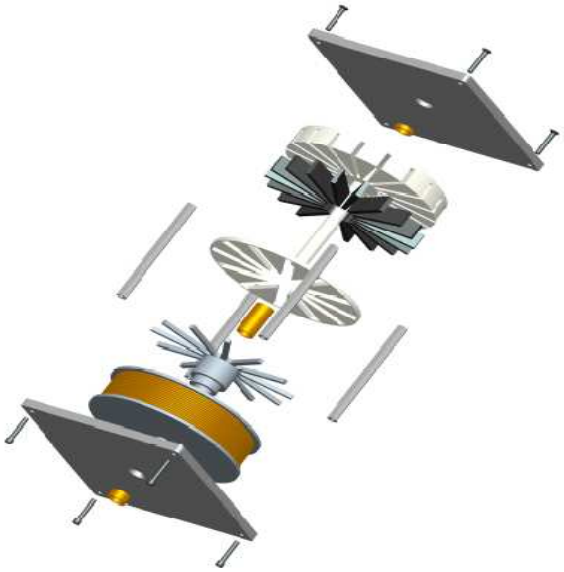

Figure 4.2 - Original Design

Although this design was worked in principle many of its components were too complex to manufacture with the time and resources of this project in mind. The stators

alone would have to be made of 10-20 separate pieces of iron and then a way of connecting these pieces would have to be created.

4.1.2 Design 2

This design is very similar to the first design only this design uses two coils instead of one coil. The two coil design is larger and it weighs more. This design is also pancake style. This design includes everything in design one with an extra coil and inner and outer poles.

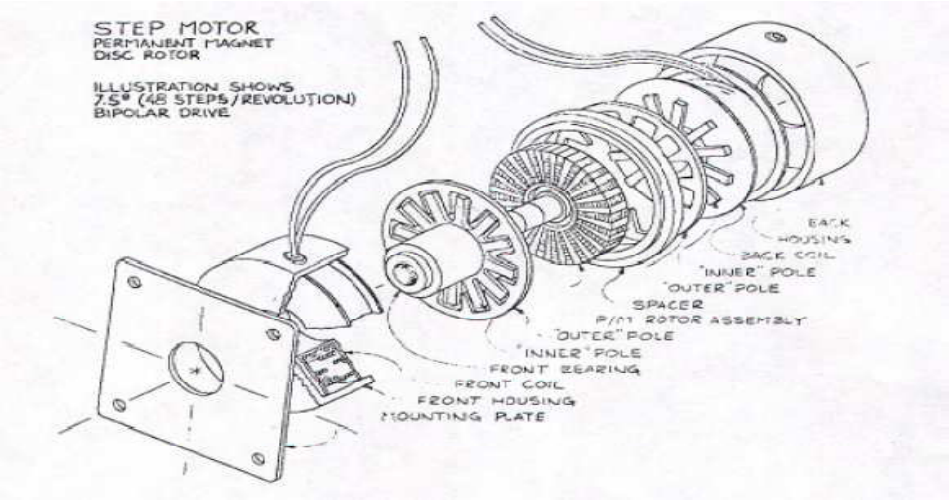

Figure 4.3 - Basis for actuator design

The advantages of the disk-rotor permanent magnet motor with 2 coils are that first the motor diameter can be made smaller than a conventional cylindrical- rotor motor having similar performance characteristics. At the same time since the poles on the rotor are magnetized in the axial direction, oriented magnetic materials may be used instead of the non-oriented materials. The oriented materials have a greater flux density which produces more torque per ampere of input current than a non-oriented material. As a result, the motor efficiency is improved. Below is a diagram of the actuator's operation principal.

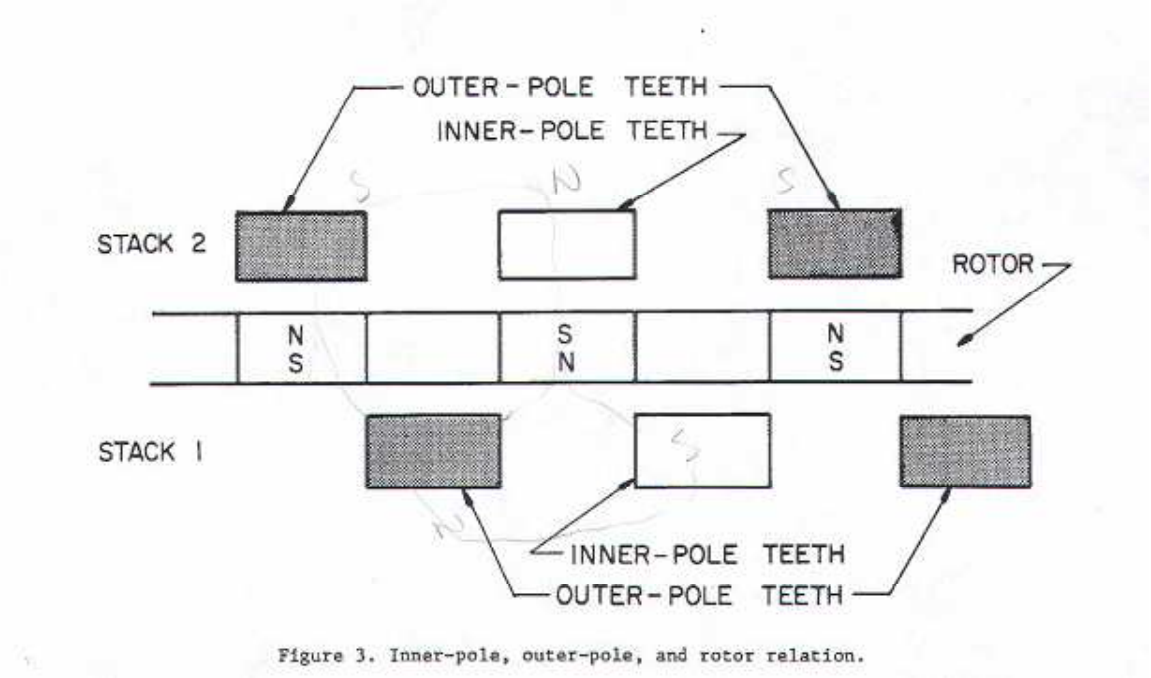

Figure 4.4 - Operation of two stator actuator

When the teeth of stack No.1 of the stator are in alignment with the rotor poles, those of Stack No.2 are in total misalignment. Thus, as the phase energization is switched from Stack 2 to Stack 1, the rotor will rotate one-half of a pole pitch of the rotor. For example, if Stack 2 is polarized to S, N, and S, the rotor remains stationary. After that, the teeth of the rotor rotate to align with the Stack 1 when Stack 1 has polarization with N, S, and N.

4.1.3 Design 3

This design contains one coil in which that coil surrounds the rotor. Many different companies currently design these actuators. The functionality is the same as the above two designs the coil and rotor are just in different orientations. This design however, does not take advantage of the maximum moment arm. The rotor radius is smaller than the actuators radius making the moment not as large as it can be for an actuator of that size.

The advantages of this design are that it dissipates much less power in losses such as heat than the cylindrical rotor and that it produces high torque and speed for its size.

The main disadvantage to this type of actuator is that it produces a smaller torque than the 2-coil type because the surrounding coil constrains the size of rotor disk. The diagram below show how this style actuator works.

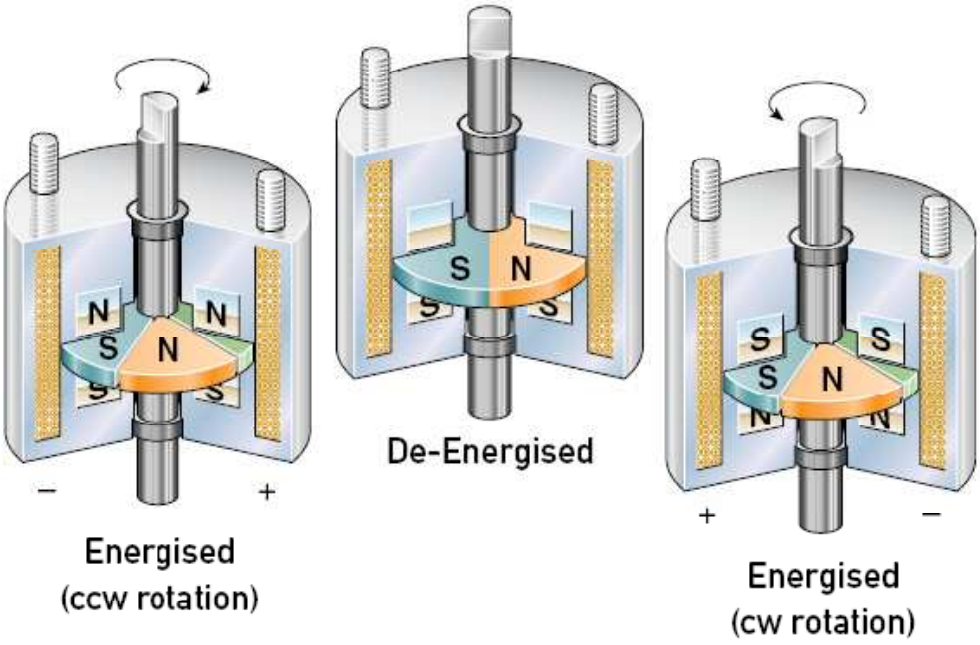

Figure 4.5 - Operation of single coil surrounding rotor

In the de-energized state, the armature poles each share half a stator pole, causing the shaft to seek mid-stroke. When power is applied, the stator poles are polarized. This attracts half and repels the other half of the armature poles, causing the shaft to rotate. When the voltage is reversed, the stator poles are polarized with the opposite pole. Consequently, the opposite poles of the armature are attracted and repelled, thus causing rotation in the opposite direction.

4.1.4 Final Design

Our final design uses one coil and two stators to apply force to the rotor. This design is by far the most compact and simple of the group, but sacrifices torque to achieve these qualities. Because of the strict requirements of our project this design is the most desirable of all the designs. Even though the torque is lower than the previous design it is still within our performance specifications.

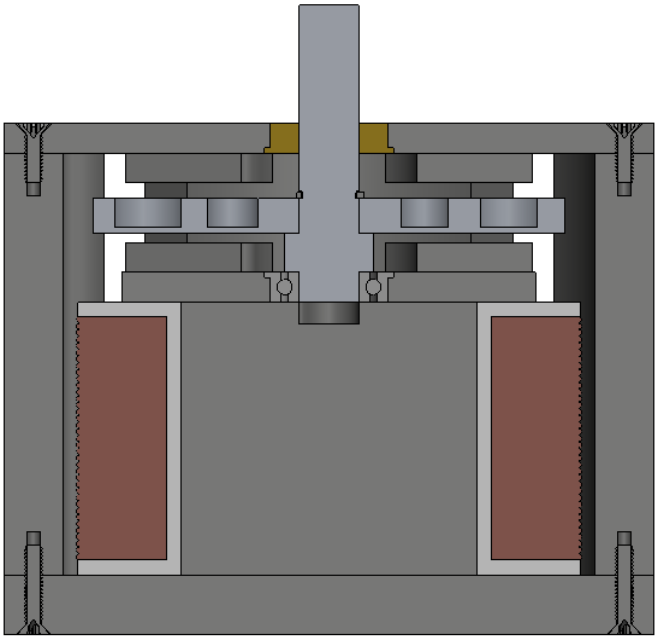

Figure 4.6 - Final design cross-sectional view

This actuator design uses principles from all of the above designs. Although it is single coil design, the outer housing is made of a magnetic material so the lower pole of the coil can be channeled to the upper stator. This effect acts as a second coil, but in order to achieve this, the current through the coil must be greater than if there actually were two coils. The operations and specifications of this design will be discussed in the following sections and appendices.

4.2 2D Modeling and Analysis

4.2.1 Maxwell 2-D Model

All of the 2-D modeling was done in Maxwell SV. Maxwell SV is the leading electromagnetic simulation software program that delivers numerical power and ease of use for analyzing electrostatic and magneto-static designs. This 2-D model was constructed after researching the principles of rotary actuators and stepper motors. First, a hand sketch was done during a teleconference with our sponsor. Once the initial

dimensions were agreed upon, the model was created using simple shaped to represent the real world actuator. The software contains the material properties to determine how a magnetic field will effect and translate through the model; therefore, each component must be assigned a material. Then, inputs and boundary conditions were established. In order to establish the flow of the current, a current source was placed in both sides of the coil. These two current sources had opposite signs indicating the direction the current was to flow. The magnetic field generated by the flowing current interacted with the surrounding materials and caused the magnets to move depending on the direction of the current. Next the executive parameter was set up. In this case the force generated between the magnets and the stators was measured. This force could then be taken and multiplied by the radius of the rotor to obtain the theoretical torque (See Appendix A). Finally, a solution had to be determined. Once a solution was converged upon, post processing graphs and output variables could be displayed.

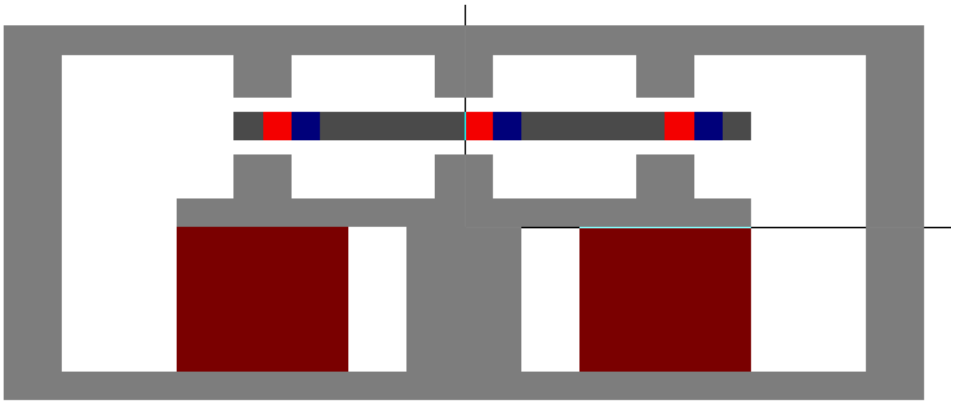

Figure 4.7 - 2D model of rotary actuator

4.2.2 Maxwell 2-D Analysis

Figure 4.8 and 4.9 show the magnitude of the magnetic field and the direction of the magnetic flux lines respectively. This is useful in determining the gaps between the components of the actuator. As can be seen in the figures below, no parts of the actuator have become magnetically saturated; this indicates that the gaps in our final design were sufficient.

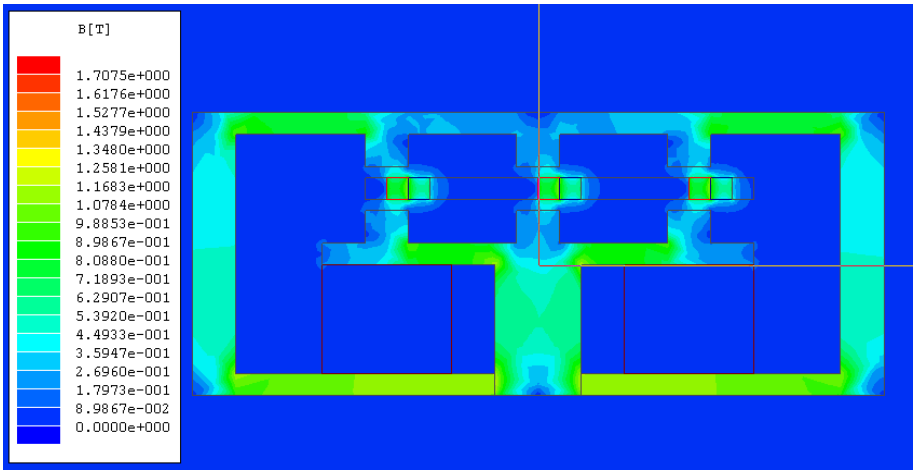

Figure 4.8 - Magnetic field magnitude plotted on surface

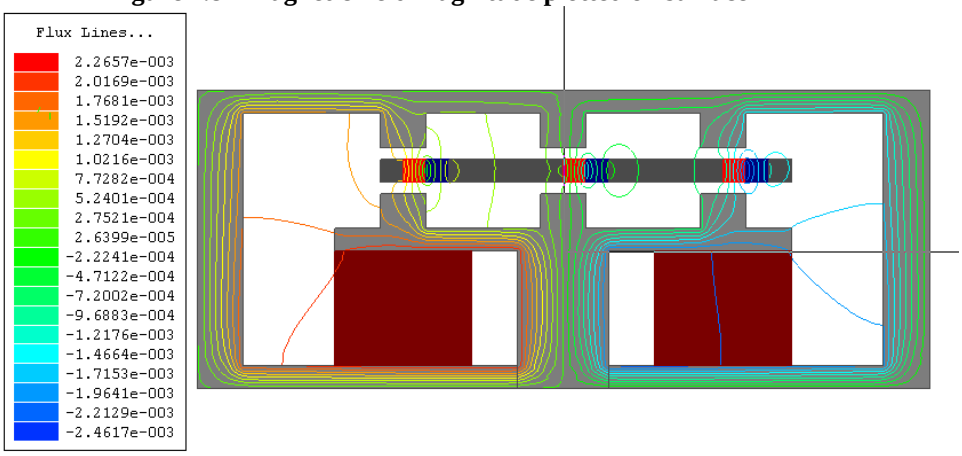

Figure 4.9 - Magnetic flux lines plotted on surface

4.3 3D Modeling and Analysis

4.3.1 Maxwell 3-D Model

The 3-D modeling was all done in Maxwell 3-D. Maxwell 3-D is software package that uses Finite Element Method for analyzing electrostatic and magneto-static designs. A 2-D model was first constructed and analyzed to use as a starting point for dimensions and other variables. Certain dimensions had to be altered significantly because the equations and variables are very different from 2-D to 3-D. Once the 3-D model was constructed, materials were assigned to the different parts. The software contains the material properties to determine how a magnetic field will effect and translate through the model. Then, excitations and boundary conditions were established.

A current was placed through the copper coil inducing a magnetic field. This magnetic field interacted with the surrounding materials and caused the magnets to move depending on the direction of the current. Next the executive parameter was set up. In this case the torque of the rotor was calculated by the software because the calculations would be too difficult to do by hand. Finally, a solution had to be determined. The number of passes the software should make and the percent of error acceptable for a solution were input. Once a solution was converged upon, post processing graphs and output variables could be displayed.

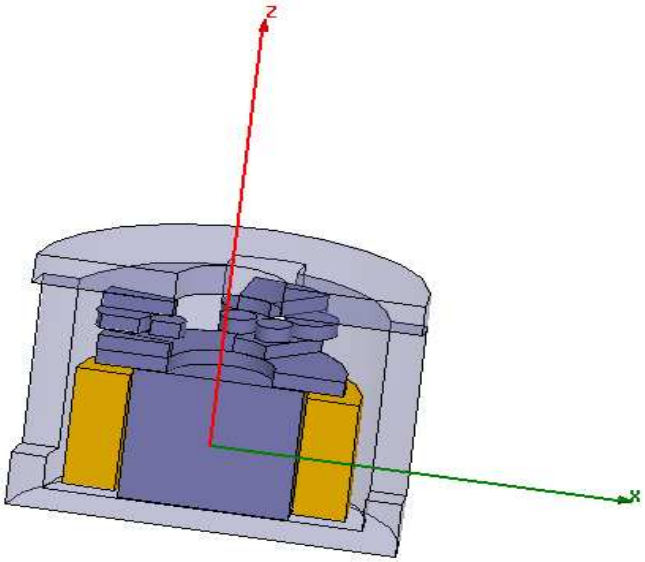

Figure 4.10 - Cross section of 3D model

4.3.2 Maxwell 3-D Analysis

Figure 4.11 and 4.12 show the magnitude of the magnetic flux in the various parts. This is useful in determining whether or not the field created by the coil will saturate any of the steel which would decrease the performance of the actuator. These figures show that no piece of the actuator is saturated and should be working at their peak performance.

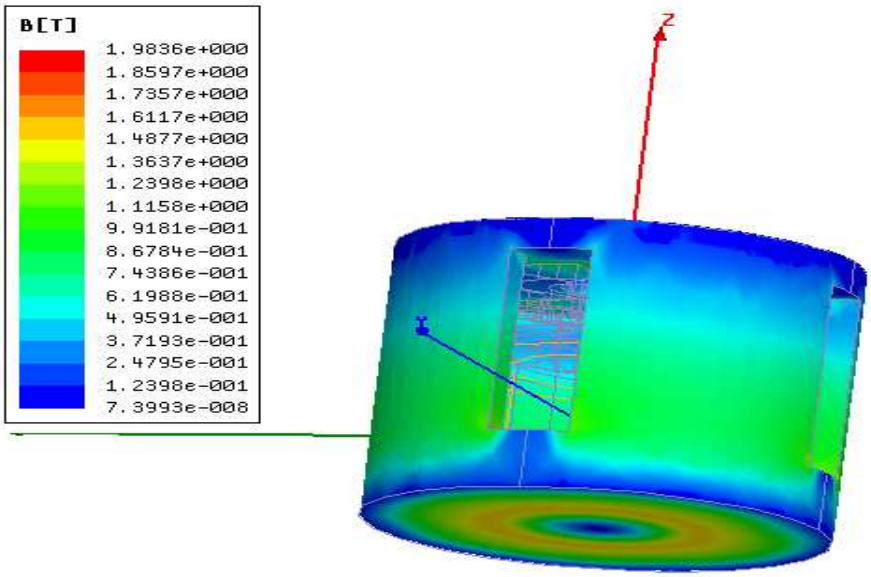

Figure 4.11 - Outer housing magnetic flux plotted on surface

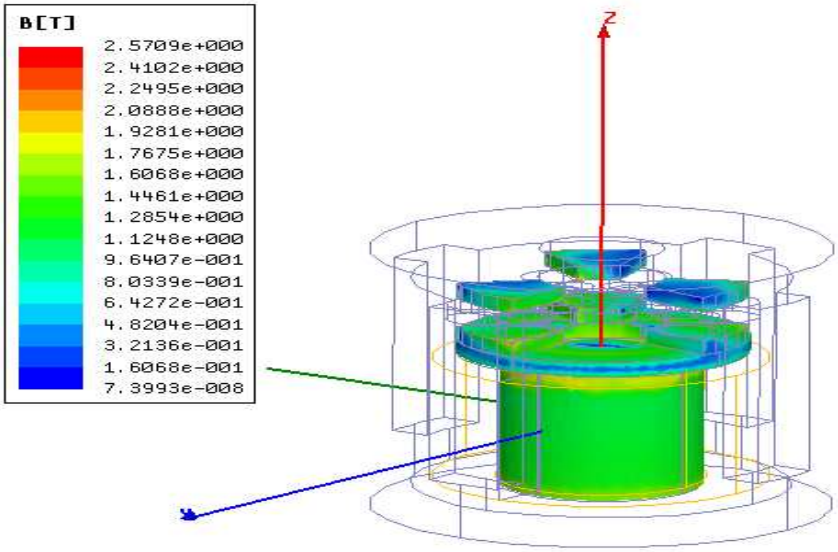

Figure 4.12 - Inner parts magnetic flux plotted on surface

The figure below shows the vector lines for the magnetic field. As it shows, the field lines start from the core of the coil and then disperse up the actuator and circle back around to the coil proving the design is functional.

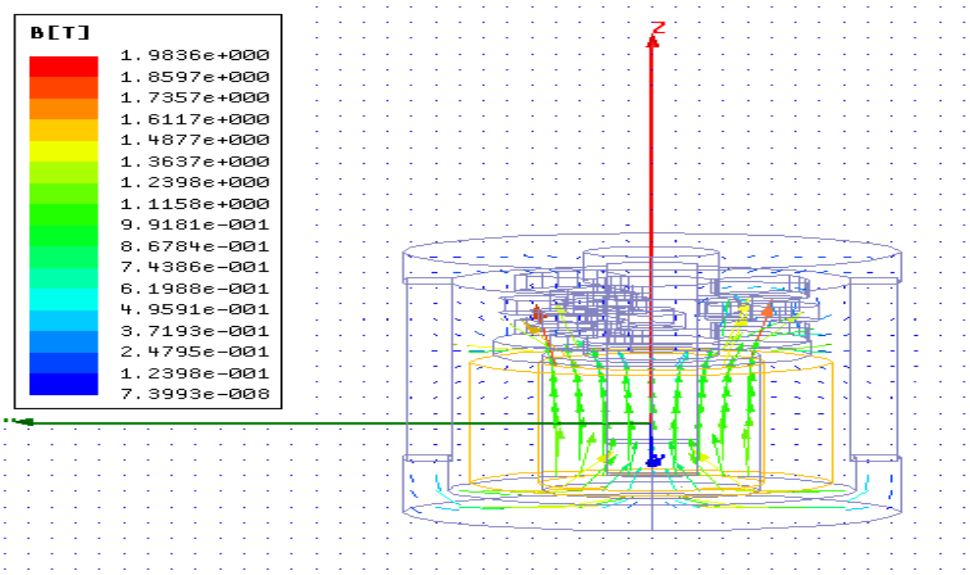

Figure 4.13 - Magnetic field lines in actuator

4.3.3 Thermal analysis on E-Physics

E-physics is a finite element software package that can determine thermal characteristics of systems. This program worked well with our design because importing the design was easy and the software is based like Maxwell 3-D. Thermal analysis is needed because the surface temperature of the actuator needs to be determined. The graph below shows the temperature distribution over the surface of the actuator. This surface temperature is important because this is the temperature that will actually be felt by other components around the actuator. The temperature distribution will be when the actuator is at steady state so these values are relatively conservative. The actual temperature might not reach the values in the picture. To also be on the safe side, four fans will be used to remove some of the heat out of the system.

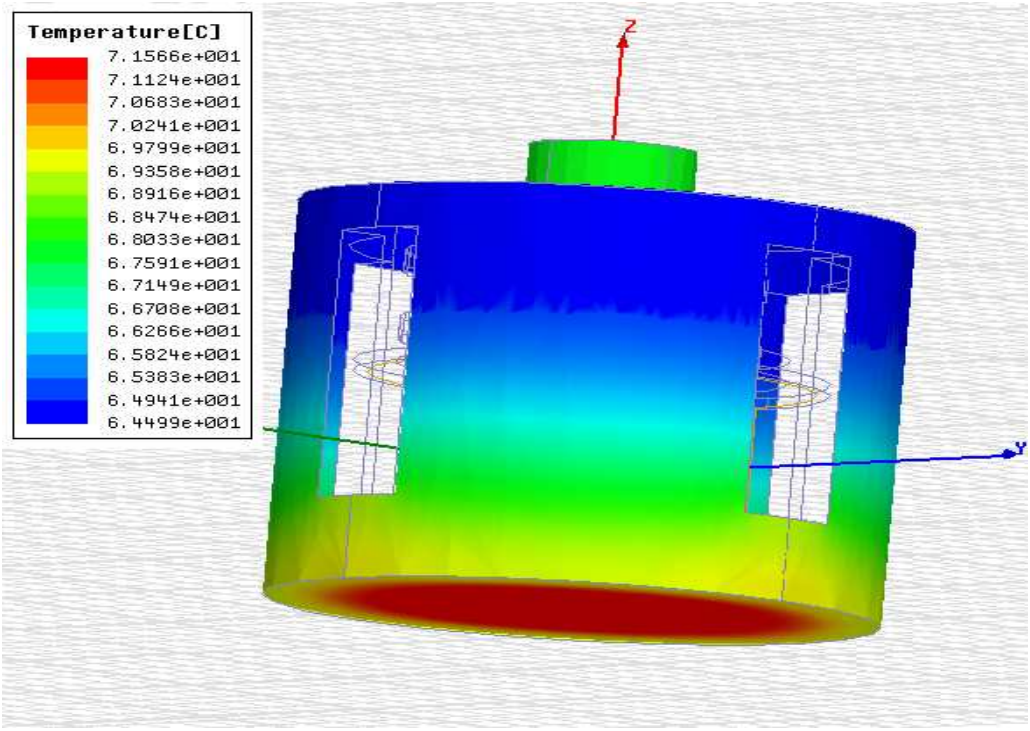

Figure 4.14 - Temperature distribution on surface of actuator

4.3.4 Optimization

The main size constraint for this project was to keep the rotor at a 2-inch diameter. This left many different parameters to be optimized to reach the desired torque of 0.3 N-m. The effect of changing a single parameter would affect the rest of the design. For instance, if the air gap was decreased to increase the magnetic field felt by the magnets, the attraction between the magnets and the stator would increase as well and that attraction must be overcome before the rotor would move. Each individual parameter was taken separately and the effects on the system were simulated. If a low torque was encountered more amp turns were added to increase the magnetic field. The higher amp turns account for higher temperatures that could potentially be hazardous if the amp turns get to high. The increase in amp turns would also increase the magnetic field that would be measured on the surfaces of the materials to determine if the material becomes saturated. If saturation occurred, the amp turns would be decreased and the magnets would be moved closer to the stators. As stated before the smaller the air gap the more torque the rotor has to overcome. In addition, the magnets have a strong magnetic field,

which increases, as the distance between decreases. This could possibly saturate the stator and the system would become useless.

There also was a problem of where to line the magnets up in a starting position. The goal was to find the position that would generate the greatest initial torque. Simulations were run at various orientations and the torque was calculated. The position with the greatest torque was when the middle of the magnets were over the sides of the stators.

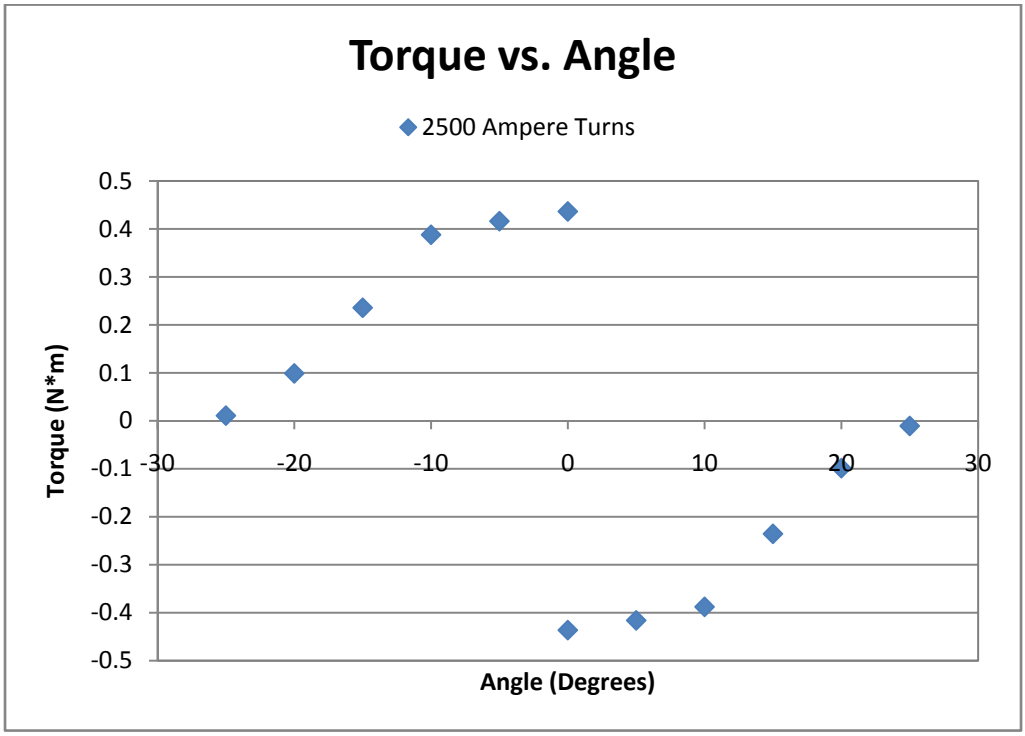

Figure 4.15 - Torque vs. magnet angle

Figure 4.15 shows when a positive or negative voltage is applied it causes the shaft to rotate clockwise (-) or counterclockwise (+). When the power is removed, the restoring torque brings it back to a neutral position. The torque decreases as the rotor turns farther because the magnets reach an equilibrium position and will no longer move. This occurs at about 30°.

4.4 Prototype

The prototype was modeled in Solidworks 2008 in order to have drawings for machining the prototype (Appendix E). Below is the Solidworks assembly as well as the exploded view of the Actuator model. Once all of the simulations were complete it was decided upon that due to thermal concerns the current in our design would be limited to 1500 ampere turns. Although this put a limit on our torque as well we were still able to achieve our goals and produce a torque of 0.41 N-m (Our goal was a torque of 0.31 N-m, see Appendix F, section II).

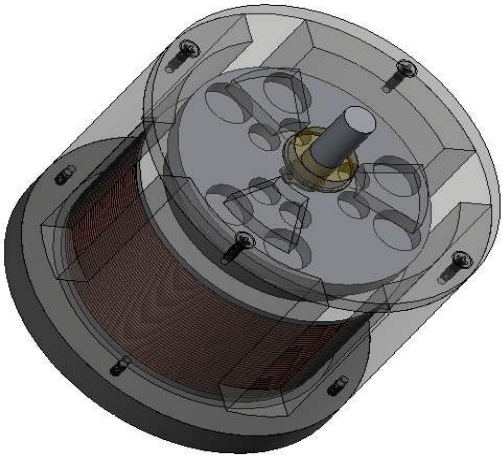

Figure 4.16 - Actuator model assembly

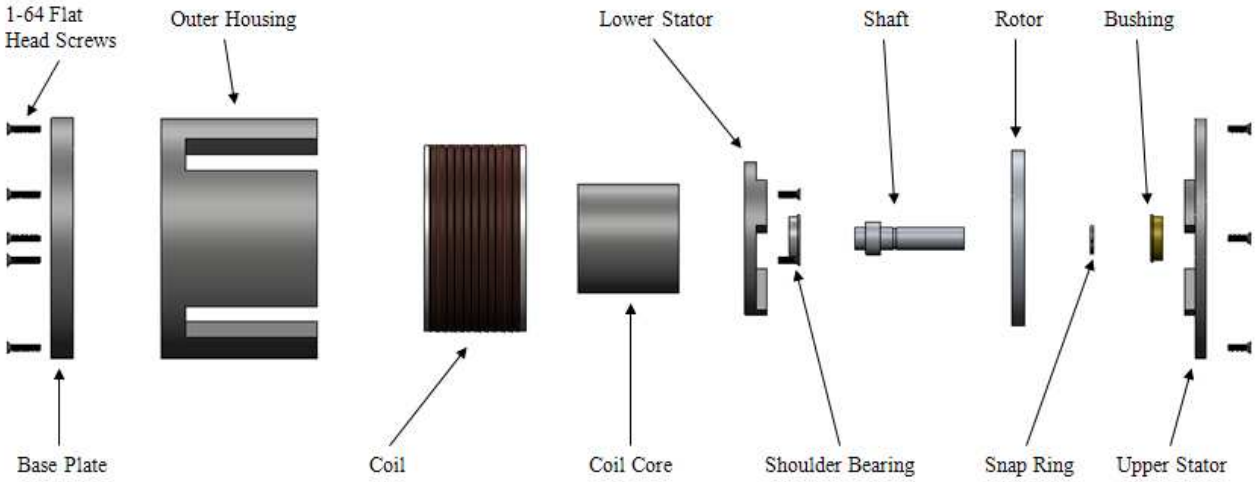

Figure 4.17 - Actuator model exploded view

4.5 Materials Selection

For the most part the materials to be used were specified by the sponsor and can be reviewed in Appendix C. These materials were used in Maxwell 2D and 3D as close as possible. Equivalent materials were chosen for materials that were not available in the software.

The housing of the model is made of 1045 Medium-Carbon Steel in order to conduct the magnetic fields from the coil and keep ease of machinability. The material acquired for the rest of motor components was as specified by the sponsor, but the shape of some components is different from the original reference motor. The shape was changed from square to round in order to more uniformly conduct the magnetic field, this results in more torque. Disc shaped NdFeB magnets are used and after many trials with the Maxwell software it was determined that we will use a mixture of 0.375 inch and 0.25 inch diameter magnets. Both sizes of magnet are 0.125 inches thick and six of each size will be embedded inside of an aluminum rotor.

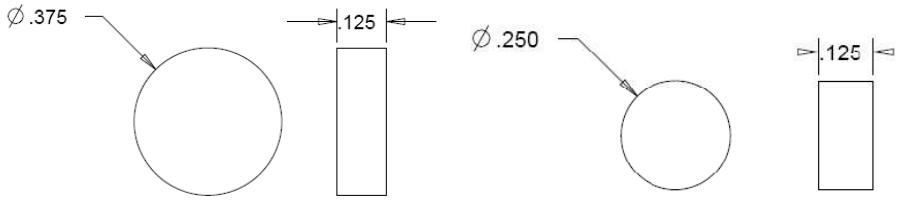

Figure 4.18 - Dimensions of NdFeB magnets in system

5 Fabrication and Assembly

5.1 Fabrication

Once all of the necessary materials arrived, fabrication of the various components required for the operation of the actuator began. During the fabrication process the Sandia team made use of the facilities at the FAMU-FSU College of Engineering; The College of Engineering graduate machine shop for the metalworking and the National High Magnetic Field Laboratory for the coil fabrication. (See table 5.1 for list of components and quantities)

PART NUMBER	PART NAME	MATERIAL	QTY.
1	Flat Head 0.375	STAINLESS STEEL	7
2	Base Plate	1045 MEDIUM-CARBON STEEL	1
3	Coil Core	1045 MEDIUM-CARBON STEEL	1
4	Spool	POLYETHERMIDE	1
5	Coil	22 GAUGE COPPER WIRE	1
6	Lower Stator	1045 MEDIUM-CARBON STEEL	1
7	Ball Bearing	STAINLESS STEEL	1
8	Housing	1045 MEDIUM-CARBON STEEL	1
9	shaft	ALUMINUM 6061	1
10	Rotor	ALUMINUM 6061	1
11	Snap Ring	STAINLESS STEEL	1
12	Bushing	BRASS	1
13	Upper Stator	1045 MEDIUM-CARBON STEEL	1
14	Flat Head 0.25	STAINLESS STEEL	7

Table 5.1 - Bill of Materials

5.1.1 Rotor and Shaft

The rotor and shaft were made out of 2 inch round Aluminum 6061 because it is easy to machine and it is non-magnetic. The first rotor had the magnet holes open on both ends and was going to be covered with caps. That design proved to be too large to fit in the entire assembly. A second rotor was made slightly larger than 0.125 inches thick to accommodate the magnets and allow them to rest in bottom. The holes were 0.325 inches in diameter along the outer radius of the rotor and 0.125 inches in diameter along the inner radius. The hole in the center of the rotor was 0.25 inches in diameter for the shaft to be press fit. The shaft was made with a shoulder 0.375 inches in diameter for the rotor to rest on. The shaft was 0.25 inches in diameter at the end to be press fit into a ball bearing as well. Its length was 1.25 inches.

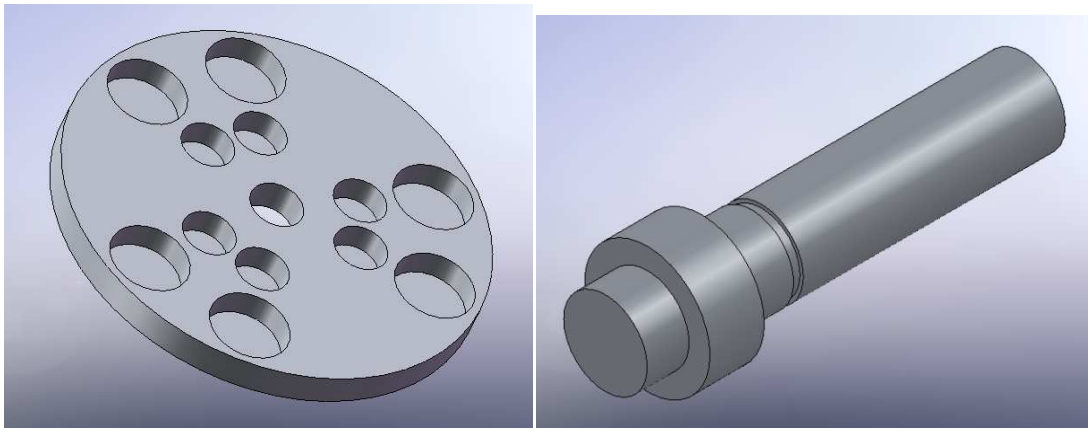

Figure 5.1 – Rotor and Shaft

5.1.2 Stators

The upper and lower stators were made from High Strength 1045 Medium Carbon Steel. It is very difficult to machine but it was used because of its magnetic properties. The lower stator was 1.75 inches in diameter and 0.125 inches thick in some areas and 0.25 inches at the poles. At 80° intervals on the stators 40° pie wedges were made to act as the poles. There were 3 of these poles on each stator. The poles were 0.125 inches high. The lower stator had a 0.5-inch diameter hole with a shoulder to have a bearing press fit into it. The upper stator was 2.75 inches in diameter with the same pole dimensions which line up with the lower stator poles. The upper stator had a hole 0.5 inches in diameter to accommodate a brass bushing to help with alignment and friction between the shaft and stator.

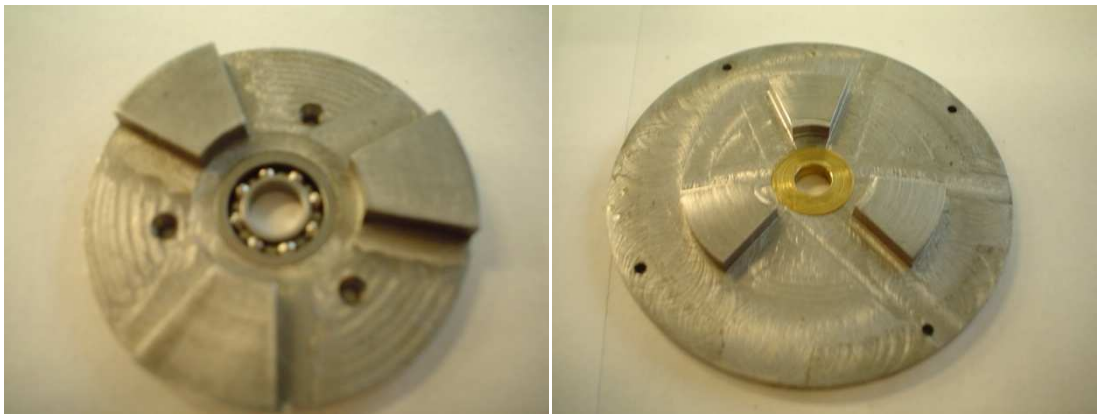

Figure 5.2 - Lower and Upper Stators

5.1.3 Base Plate and Housing

The base plate and housing were also made out of Steel due to its magnetic properties. The base plate was 2.75 inches in diameter and 0.25 inches thick. The thickness had to be just right to prevent saturation of the steel as well as to transport the magnetic field. The housing was a hollow cylinder with height 1.78 inches and wall thickness of 0.25 inches. There were also four slits cut into the sides of the cylinder to improve airflow and make room for the copper wires to come out. These slits were 0.5 inches wide and 1.5 inches high.

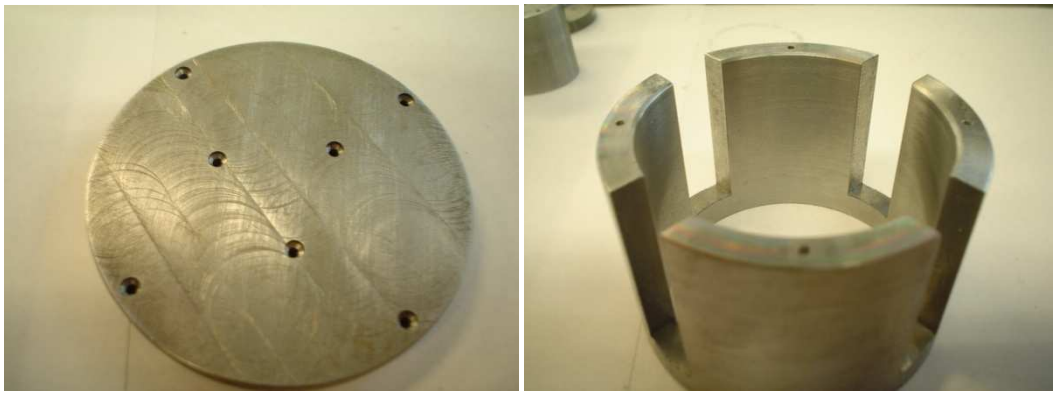

Figure 5.3 - Base plate and Housing

5.1.4 Spool and Coil Core

The spool was made from Polyetherimide, a high temperature plastic. The high temperature plastic was needed to assure that the spool would not melt from the temperature of the coil. The Spool was 2.125 inches in diameter at the top and bottom with a 1.0875-inch diameter in the center where the copper wire was wrapped. A 1.25-inch hole was in the middle of the spool to accommodate the coil core. The coil core was made out of Steel and it was a cylinder 1.25 inches in diameter and 1.15 inches high.

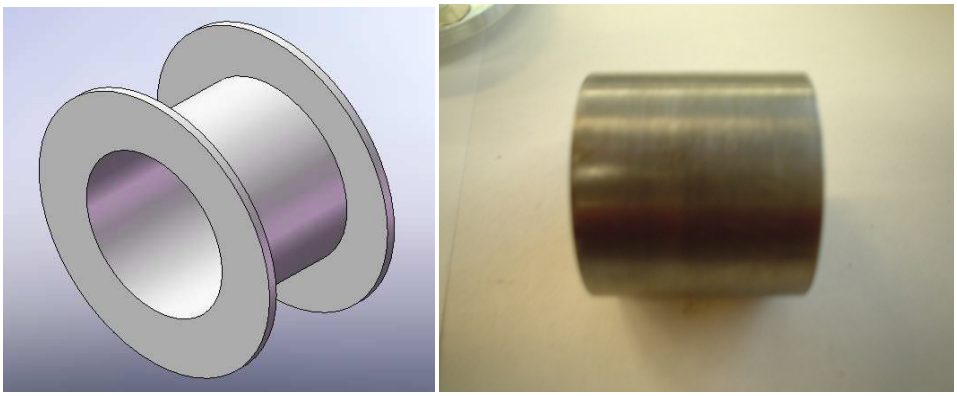

Figure 5.4 - Spool and Coil core

5.1.5 Winding Fixture Fabrication

In order to wind the copper wire around the spool, it was necessary to make a winding device. This device fixed the spool to the winding lathe. A 0.25-inch steel rod was used for the shaft. There was another steel rod used, which has the same diameter as the hole in the middle of the spool, so the spool was prevented from moving around by fitting the rod into the hole of the spool. A nut was also welded on the shaft to support the washer. To support the spool, washers were used on the both side of the spool. At the end of the shaft, another nut was used to tighten the winding device.

Figure 5.5 - Winding fixture parts

5.1.6 Coil Fabrication

For the winding process, 232 feet of an insulated copper wire were used. There were a total of 504 turns around the spool and about 35 turns per layer. In addition, the

winding device was applied to fix the spool to the lathe during the winding process. The steel rod and shaft were inserted in the spool, and the nut was tightened. Then, the device holding the spool was set up on the lathe. For the first turn of the first layer, a plastic sheet was used to keep the wire free because the spool could not have holes for the inlet and outlet of wires. In addition, a Teflon tube was used to cover the lead wire to keep it from shorting out. For the first couple of layers, it was required to ensure to compact the winding layer with 35 turns at each layer. After 504 turns, it was finished with epoxy tape to prevent from unwinding.

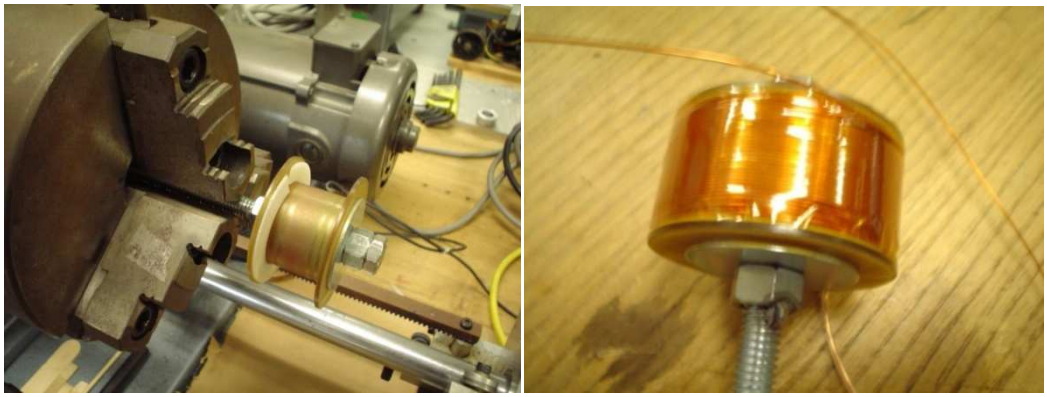

Figure 5.6 - Spool on winding lathe (left) and Completed Coil (right)

6 Assembly

6.1 Assembly

The full assembly of the rotary actuator consisted of two minor assemblies, the rotor assembly and the housing assembly

6.1.1 Rotor Assembly

Originally, the design for the rotor was to have the holes for the magnets go through the entire rotor. Then, caps covered the magnets to keep them in place. These caps proved to be too large for the assembly to work. The logical solution was to remove the caps and try it without them. The magnets were still held in place from the adhesive used for the caps. Unfortunately, the adhesive was not distributed evenly and the rotor was unstable. It leaned to a side and when energized would stick to a stator. This was when a new rotor had to be designed.

The new rotor required six permanent magnets. Instant adhesive was use to fix the permanent magnets into the holes of the rotor frame. Larger magnets were located along the outer circle; smaller ones were located along the inner circle. The polarities of the adjacent magnets alternated. After adhesion, the rotor assembly was left to dry for several hours. The rotor rests on a shoulder on the shaft to keep the appropriate spacing between the lower stator and the magnets. The rotor was press fit onto the shaft and the shaft was press fit into a shoulder bearing in the lower stator. A snap ring was used above the rotor for additional support.

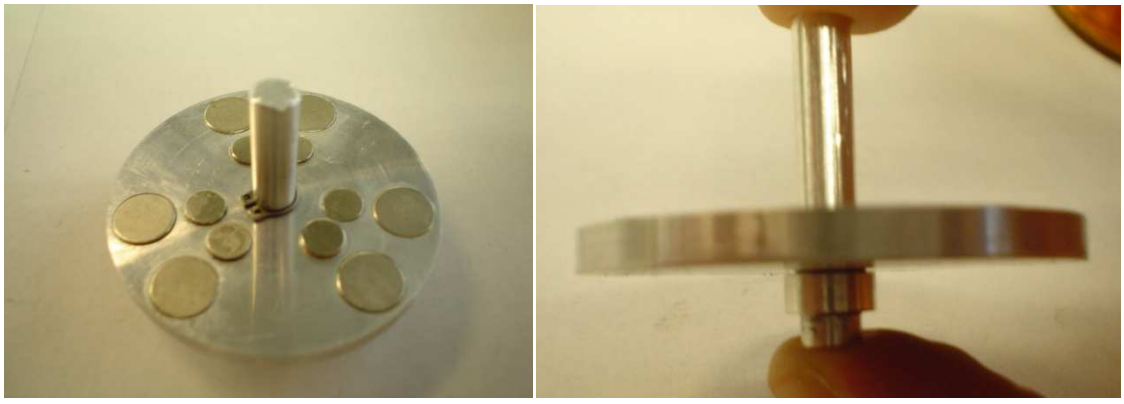

Figure 6.1 - Completed rotor sub-assembly

6.1.2 Full assembly

After the rotor assembly and the coil winding were accomplished, the full assembly was performed. At first, the coil core was attached with 1-64 flat head screws on the base plate. The coil core was inserted to the coil. Next, the shoulder bearing was press fit into the hole on the lower stator. The lower stator was then fixed with 1-64 flat head screws on the top of the coil core. Then, the rotor assembly was press fit onto the bearing in the lower stator. Once the inner components were attached and functional, the outer housing was connected to the base plate. Lead wires from the coil were put through the gaps in the housing for the testing. Finally, the upper stator was attached on the top of the outer housing with the 1-64 screws after the bushing was mounted on the upper stator.

Figure 6.2 - Fabricated parts

Figure 6.2 shows the assembled base plate and coil core. They were attached using three (3) 1-64 flat head (82°) screws.

Figure 6.3 - Base plate and Coil core

The coil assembly is then slid on the coil core. No screws or glue are needed to keep the coil in place. The lower stator will keep it from moving.

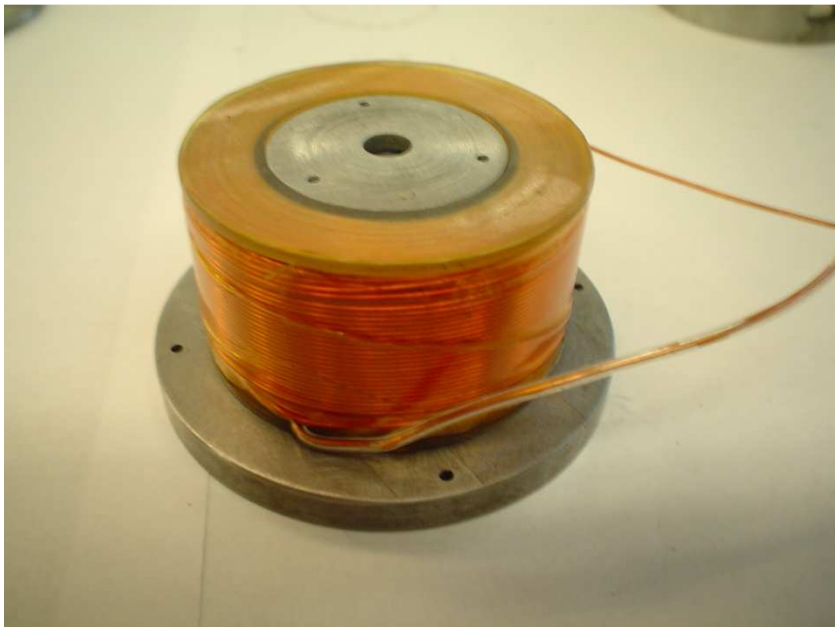

Figure 6.4 - Coil added

Figure 6.4 shows the lower stator assembly. The lower stator has a shoulder bearing press fit into it. The lower stator is screwed into the coil core using three (3) 1-64 flat head (82°) screws.

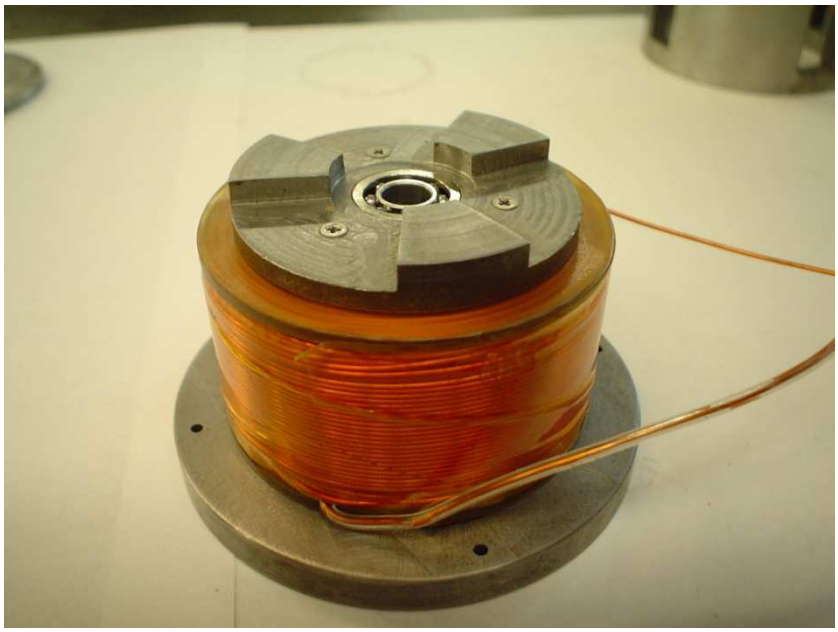

Figure 6.5 - Lower stator added

The outer housing is then attached to the base plate using four (4) 1-64 flat head (82°) screws.

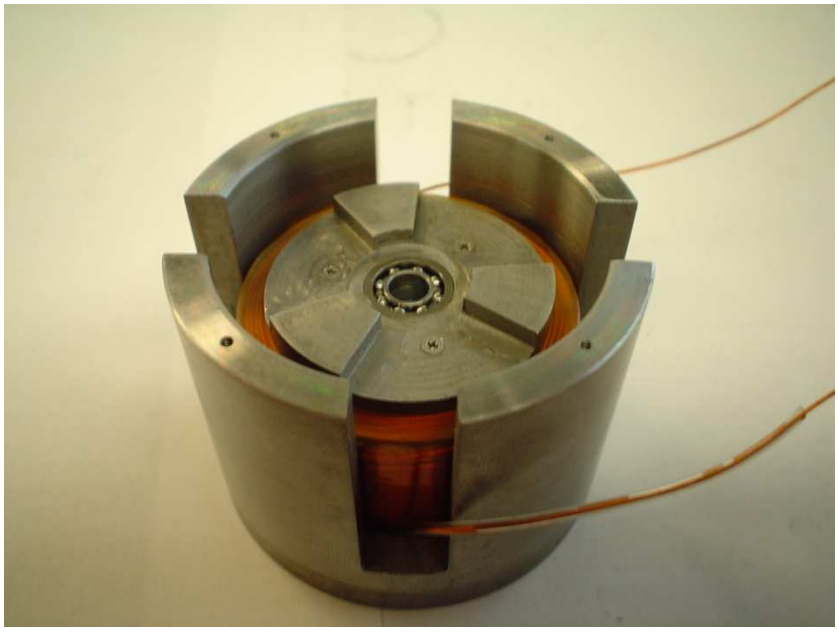

Figure 6.6 - Outer Housing attached

Next, the rotor assembly is press fit into the shoulder bearing in the lower stator. The rotor should align itself with the stators.

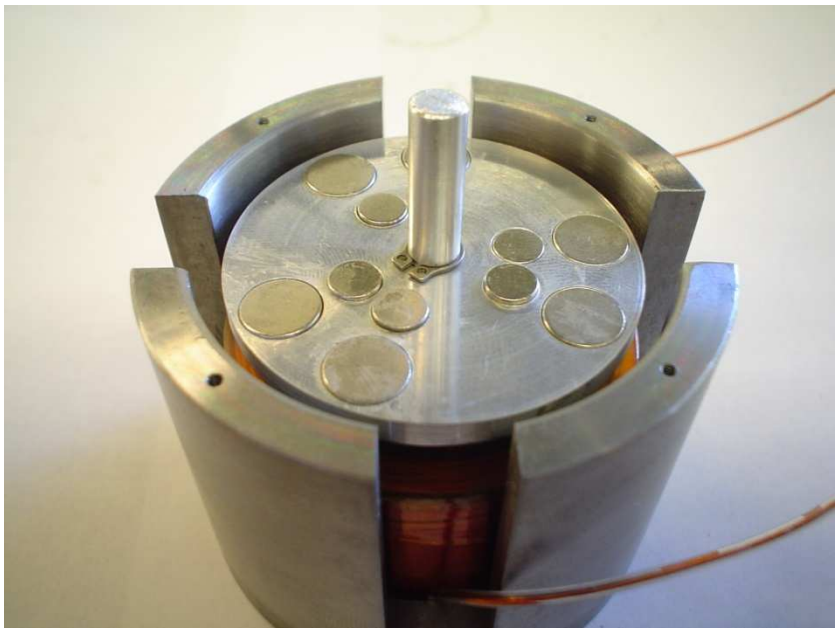

Figure 6.7 - Rotor assembly added

Lastly, add the upper stator with the brass bushing. It will snap down due to the magnetic field so be sure the stators are aligned with the lower stators. The upper stator is attached using four (4) 1-64 flat head (82°) screws.

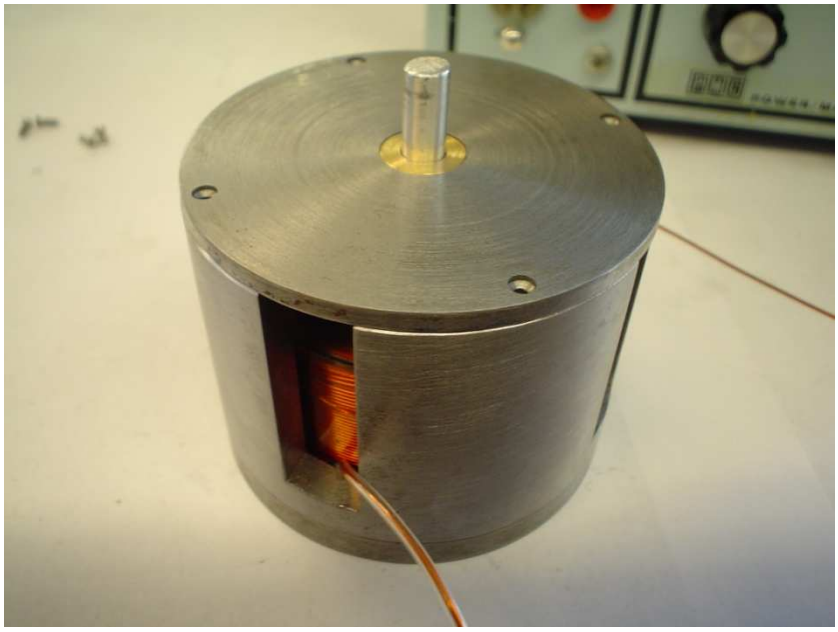

Figure 6.8 - Fully assembled actuator

7 Testing

7.1 Testing

After fabricating and assembling the actuator, it was necessary to test it and record the data. First off, a test of functionality was performed to see if the design actually worked. The next test was a thermal test to determine if the coil temperature would reach levels that would be hazardous. Lastly, attention was focused on the degrees of the steps and the amount of torque produce. Therefore, a torque test was performed.

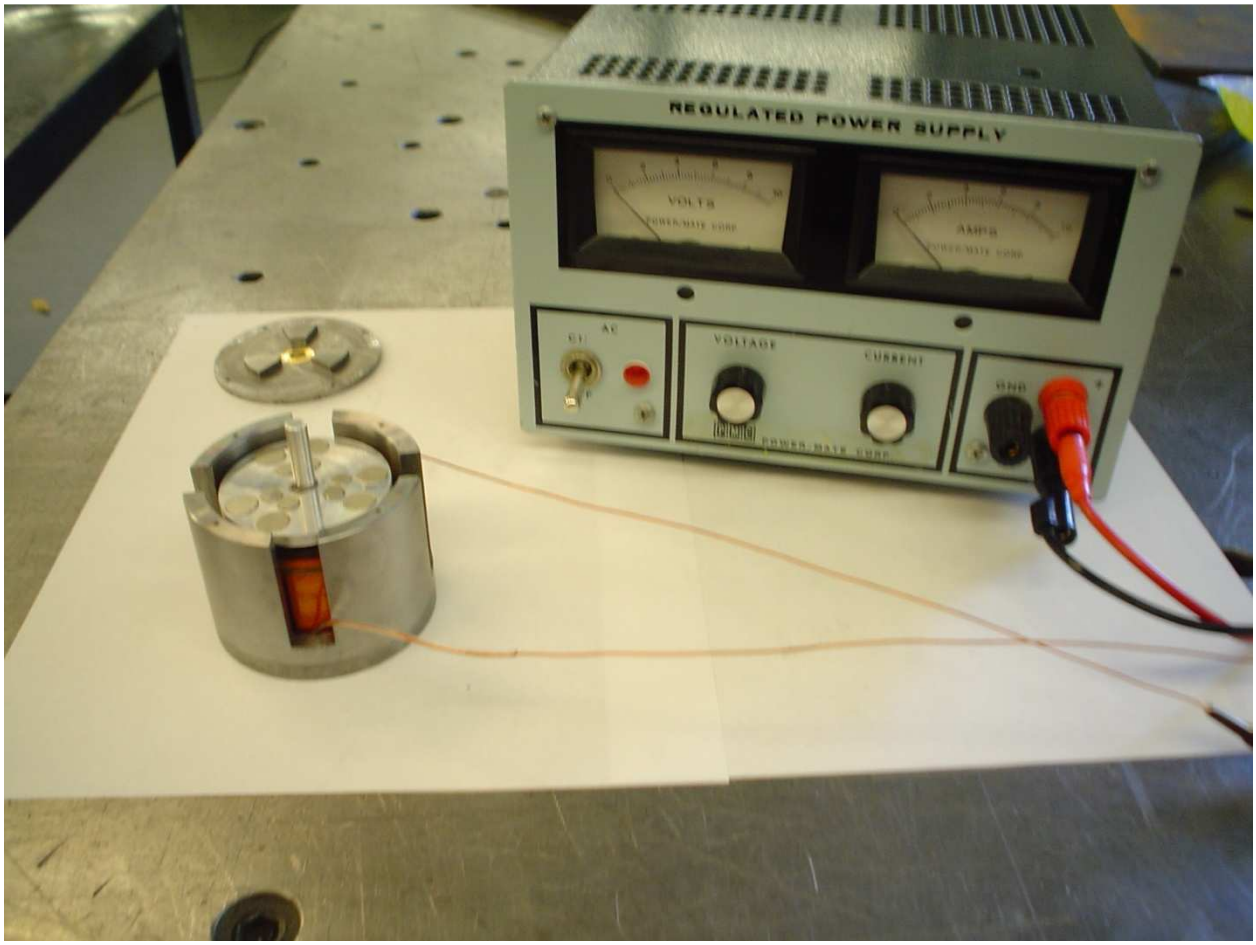

Figure 7.1 - Testing setup

7.1.1 Thermal testing

The coil made by the team at the MagLab had a coil resistance of 4.1 Ohms. Connecting the power supply to the coil and providing power to it would produce an

increase in temperature. Using computer software called E-physics, it was estimated that the maximum temperature that the mechanism would reach was 75°C. Further actual testing needed to be executed. The power supply and the coil were set up and temperature readings were measured. The temperatures were measured using an infrared thermometer. The result given by this test were quite promising for our project; after two minutes of running power through the coil the temperate recorded was 47.4°C and after five minutes the temperature reached only 53.2°C. Ideally, it only takes a second of power supply to run the actuator, so five minutes could be considered steady state in our case. Even so the temperature is acceptable for people to manipulate with minimal protection. Moreover, for safety reasons the coil was run for longer time and it did not reach the maximum temperature estimated by the software.

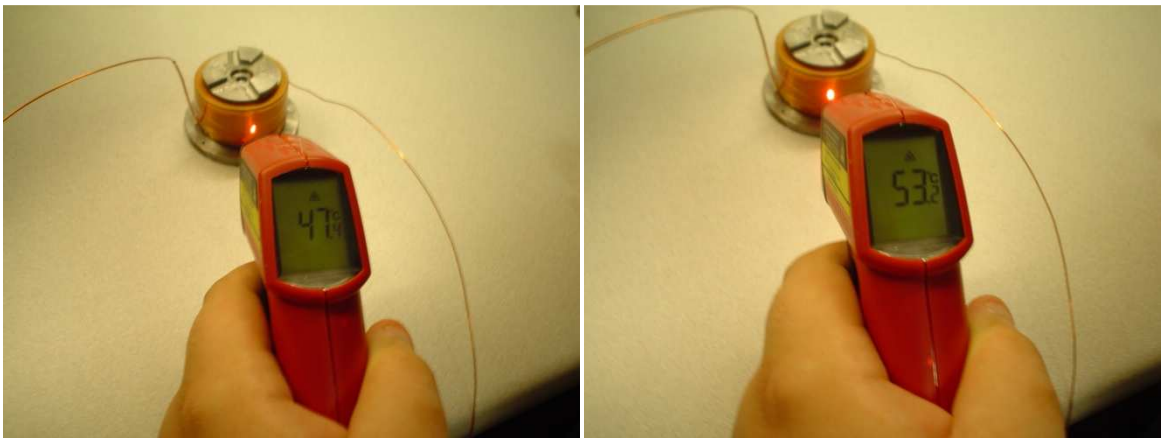

Figure 7.2 - Thermal Testing after 2 min. 47.4°C (left) and 5 min. 53.2°C (right)

7.1.2 Torque Testing

The first time the coil was connected to the power supply the mechanism did not function by any means. After realizing that the copper wire had an insulated layer and it was not making contact with the alligator clips, the issue was resolved and the mechanism began working. Quickly it was notice that running the motor without all the components attach would negatively affect the performance of the actuator. A weakness in torque was easily noticeable when actuator was partially assembled. For torque measurement, a torque gauge was used. The gauge was attached to the shaft and power was supplied to the coil, the device recorded 0.068 N-m. That value was only around one-fifth of the 0.31 N-m torque required by our sponsor at Sandia National Laboratories. The

torque results obtained during the test were by using a power supply providing around 2.5 Amperes and 10.50 Volts. A stronger power supply would produce a larger torque.

Figure 7.3 - Torque test

8 Conclusions and Recommendations

8.1 Conclusions

In conclusion, the design of the bi-directional actuator was proven correct. It was possible to design and fabricate a single solenoid that produced two directions of rotation. The direction of the current determined the direction of the rotation. When the coil was energized, the stators were magnetized with a certain polarity. The alternating polarity of each set of adjacent magnets were either repelled or attracted to the stator. The angle between the adjacent magnets was 40°. When one pair of magnets aligns with the stators, they would move half the distance, 20°. When the power is off, the rotor returns to a neutral position because both pairs of magnets were attracted to the stators.

The required torque, 0.31 N-m was not reached. The experimental torque test revealed that our device had approximately 1/5 of that torque, about 0.068 N-m. The smaller torque could be attributed to the magnets being too powerful and too close to the stators. That is to say, a greater torque had to be overcome to move the magnets off the stators. This is evident because the return torque was a greater value than the energized torque. It was also noted that the effectiveness of the actuator was slightly hindered when the upper stator was attached. This could be accounted for by the reason stated above. The magnets had to overcome two sets of stators rather than one, which slightly decreased the torque. However, the outer housing proved to be very useful in distributing the magnetic field. When tests were done without the housing, the rotor had decreased effectiveness.

Computer simulations using E-Physics calculated a maximum temperature of 75°C. This high temperature warranted a heat removal system. Thermal tests showed that the maximum temperature after 5 minutes was 53.2°C. This concluded that no heat removal system was needed because the device would not be on for that long a period.

8.2 Recommendations

As for further research on this subject, there are some recommendations to consider. It is recommended that less powerful magnets be used to account for the strong attraction between them and the stators. This strong attraction reduces the torque significantly. Next, the housing could be made with three walls as opposed to the four used in this project. The walls should line

up with stators to perhaps increase effectiveness. For the rotor and shaft, it is recommended that it be made of one solid piece rather than multiple parts to account for tolerance and assembly issues.

8.3 Acknowledgements

We would first like to thank Sandia National Laboratories, Gilbert Benavides, for sponsoring this project. His knowledge and expertise really helped us to arrive at a final product. In addition, we would like to thank Dr. Philippe Masson and Dr. Ongi Englander for their guidance. They were both very instrumental in all aspects of the project. Next, we would like to thank the Graduate Machine Shop and its staff for help with the fabrication of the actuator. Finally yet importantly, we would like to thank Mr. Lee Marks at the NHMFL for his assistance while fabricating the coil.

Appendix A: Calculations

2D Force and Torque Calculations

The radius of the rotor $r := 1in$

Force given by Maxwell software $F := 16.995N$

The torque can be estimated by $\tau := F \cdot r$

Estimated torque $\tau = 0.432\,N \cdot m$

Wire Diameter and Length

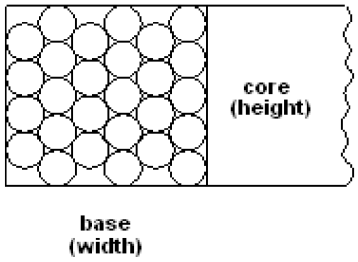

$ID := 1.25in$ $OD := 2in$ $h := 1in$

$w := \frac{OD}{2} - \frac{ID}{2}$ $w = 0.375\,in$

$A_{cross} := w \cdot h$ $A_{cross} = 0.375\,in^2$

$D_{wire} := \frac{h}{40}$ $D_{wire} = 0.025\,in$

A 22AWG wire has a diameter of 0.254in, this is close enough to our calculated diameter

Number of turns $N_{turns} := 504$

$L(t) := \lceil 2 \cdot \pi \cdot (0.70 + 0.0251 \cdot t) \rceil in$

$L := 40 \cdot (L(0) + L(1) + L(2) + L(3) + L(4) + L(5) + L(6) + L(7) + L(8) + L(9) + L(10) + L(11) + L($

$L = 2.779 \times 10^3\,in$

$L = 231.594\,ft$

The length of copper wire that we will need is 232ft

$A_{wire} := \pi \cdot \left(\frac{D_{wire}}{2} \right)^2$ $A_{wire} = 4.909 \times 10^{-4}\,in^2$

$\rho_{copper} := 0.322 \frac{lb}{in^3}$

$V_{wire} := A_{wire} \cdot L$ $V_{wire} = 1.364\,in^3$

$mass_{wire} := V_{wire} \cdot \rho_{copper}$ $mass_{wire} = 0.199\ kg$

$weight_{wire} := mass_{wire} \cdot g$ $weight_{wire} = 0.439\,lbf$

The wire used in our system will weigh 0.439 lbs

Current Density and Power Supply Requirements

Current in the coil (Ampere turns) $I_{coil} := 1500A$

Resistivity of Copper $\rho := 1.67 \cdot 10^{-8} \Omega \cdot m$

Current Density is given by $J := \frac{I_{coil}}{A_{cross}}$ $J = 6.2 \frac{A}{mm^2}$

A current density above 5 indicates that activate cooling is needed. This is an acceptable solution up to 10.

Resistance of wire $R := \frac{\rho \cdot L}{A_{wire}}$ $R = 3.722\ \Omega$

Power Supply current required $I_{supply} := \frac{J \cdot A_{wire}}{\frac{\pi}{4}}$ $I_{supply} = 2.5\ A$

Power Supply voltage required $V := I_{supply} \cdot R$ $V = 9.306\ V$

Heat Generated by Coil $P := I_{supply}^2 \cdot R$ $P = 23.265\ W$

3D Torque Calculations

Number of turns $N_{turns} := 504$

Air gap between stator and magnets $d := 0.3125in$

Permeability of Air $\mu_o := 4 \cdot \pi \cdot 10^{-7} \frac{T \cdot m}{A}$

Permeability of Iron $K_{m_iron} := 0.377$

$\mu := K_{m_iron} \cdot \mu_o \qquad \mu = 4.738 \times 10^{-7} \frac{kg \cdot m}{s^2 \cdot A^2}$

Using the magnetic flux equations and force equations we can estimate the 3D torque using the following formula

$$\tau := r \cdot \mu \cdot N_{turns} \cdot \frac{I_{supply}^2}{d} \cdot 2 \cdot L$$

The estimated torque is $\tau = 0.674\,N \cdot m$

This Torque is slightly higher than what we were able to achieve in our 3D simulations. I
real world conditions that are not taken into account by the above equations, the torque gi
is ideal.

Current Density and Power Supply Requirements using measured values

$D_{wire} := 0.0253in$ $A_{cross} := 0.375in^2$

$A_{wire} := \pi \cdot \left(\frac{D_{wire}}{2} \right)^2$ $A_{wire} = 5.027 \times 10^{-4} in^2$

Current in the coil (Ampere turns) $I_{coil} := 1500A$

Resistivity of Copper $\rho := 1.67 \cdot 10^{-8} \Omega \cdot m$

Current Density is given by $J := \frac{I_{coil}}{A_{cross}}$ $J = 6.2 \frac{A}{mm^2}$

Measured Resistance of wire $R_{actual} := 4.1\Omega$

Power Supply current required $I_{supply} := \frac{J \cdot A_{wire}}{\frac{\pi}{4}}$ $I_{supply} = 2.56\ A$

Power Supply voltage required $V := I_{supply} \cdot R_{actual}$ $V = 10.497\ V$

Heat Generated by Coil $P := I_{supply}^2 \cdot R_{actual}$ $P = 26.877\ W$

Appendix B: Graphs

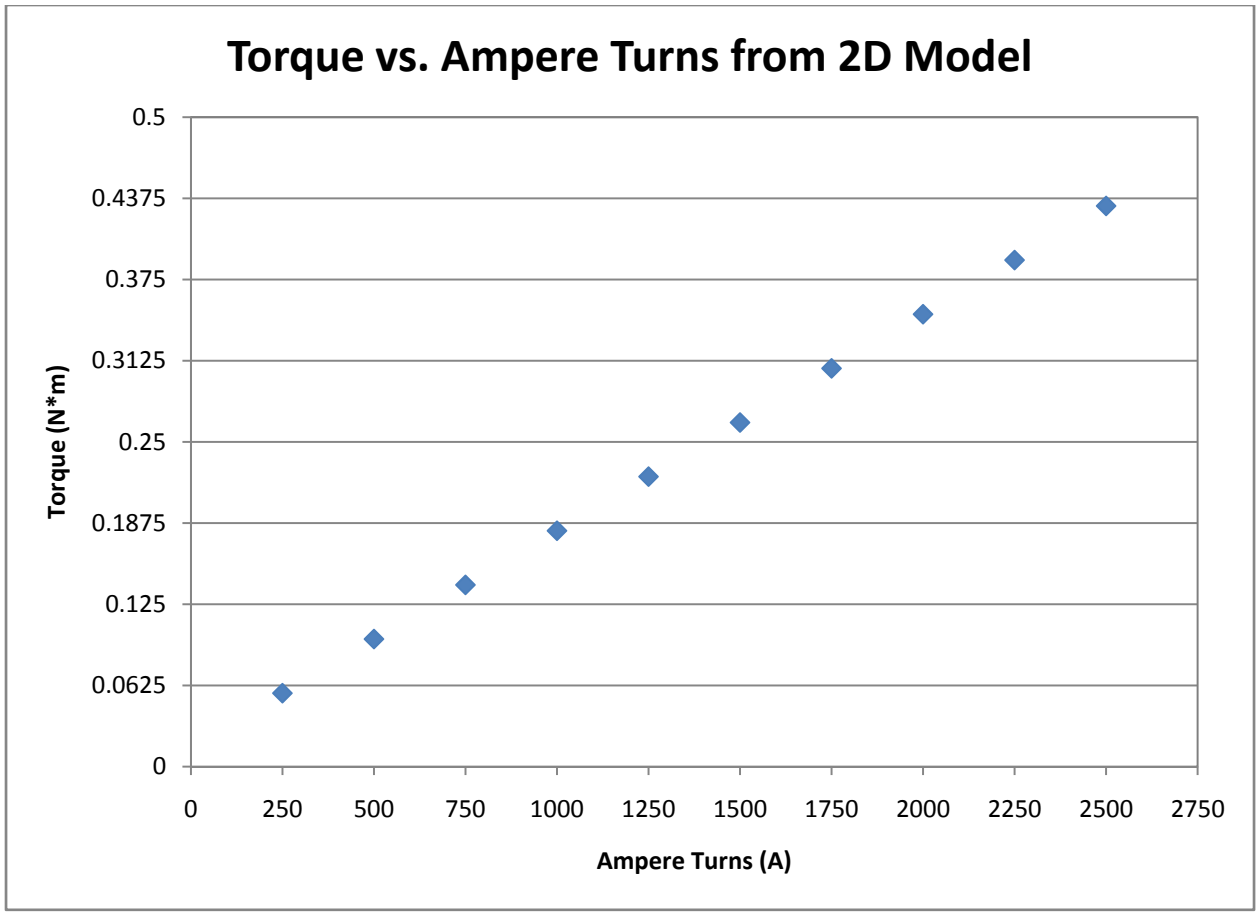

The graph above shows how the torque between the magnets and the stators changes as the total current in the coil is increased. This graph was created using data gathered from a Maxwell 2D simulation of our final design. All of the parameters were held constant except for the current in the coil. Although the torque increases with the current there will come a point where the entire device will become magnetically saturated and the torque begin to drop off and eventually go to zero.

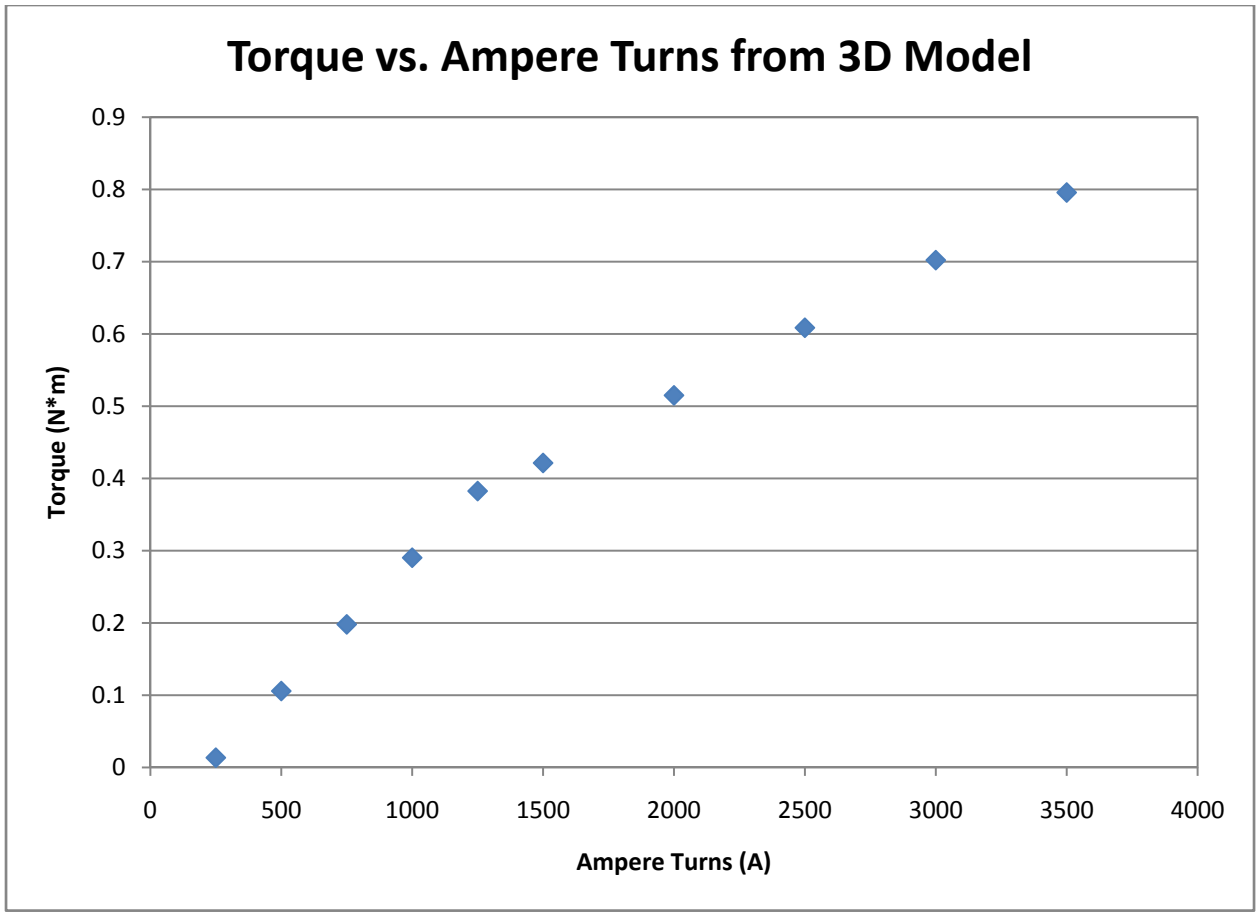

The graph above shows how the torque between the magnets and the stators changes as the total current in the coil is increased. This graph was created using data gathered from a Maxwell 3D simulation of our final design. All of the parameters were held constant except for the current in the coil. Although the torque increases with the current there will come a point where the entire device will become magnetically saturated and the torque begin to drop off and eventually go to zero. As you can see this graph is slightly different from the one above, in the 3D simulation the round shape of our device is taken into account, which changes the magnetic flux throughout the housing of the actuator. This change in magnetic flux results in a slight difference in the calculated torque.

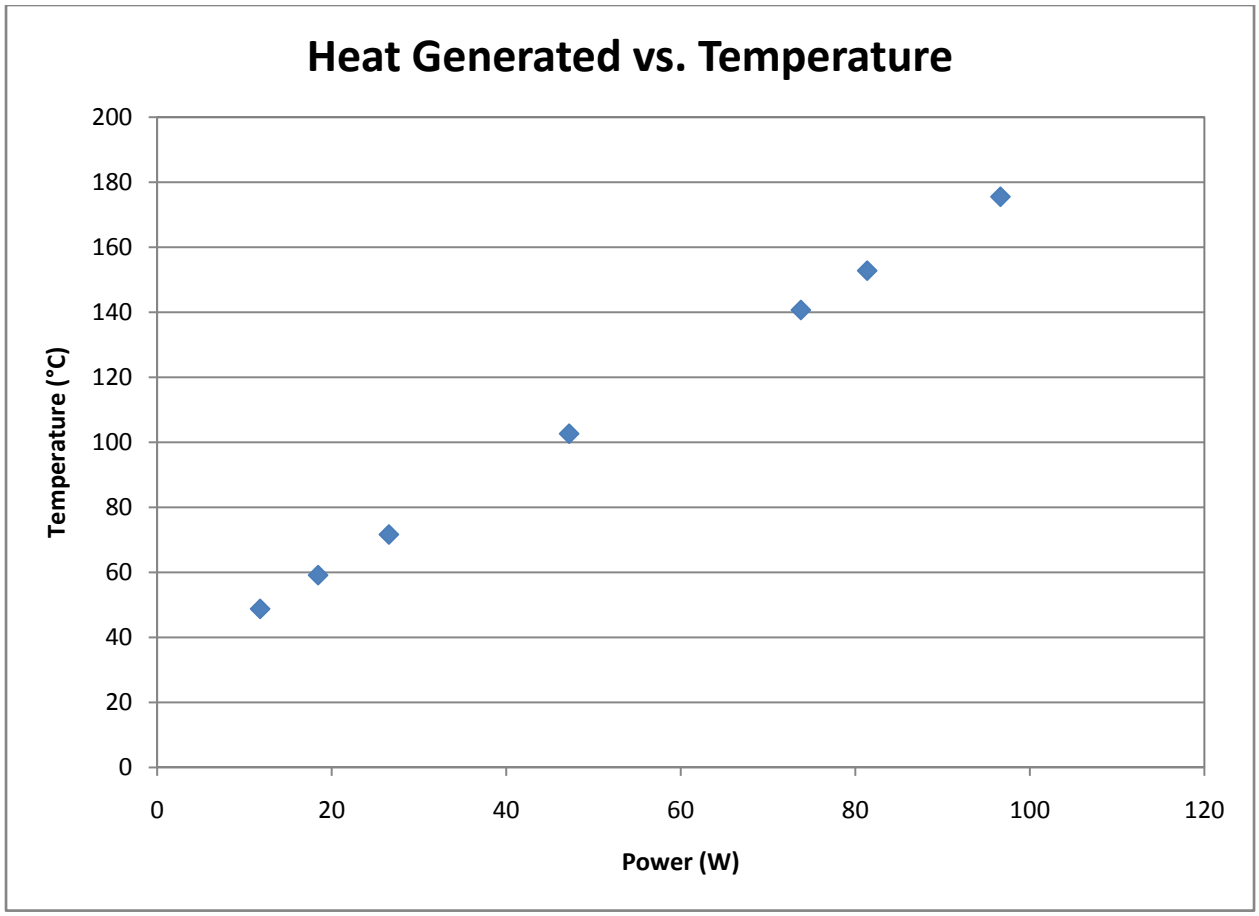

This graph shows how the surface temperature of the housing of the actuator changes with respect to the heat generated by the coil. Ideal thermal assumptions were made in order to simulate these temperatures; also, much of the actuator's internal geometry was simplified in order to simulate using the available software. To create this graph we imported our 3D model from Maxwell into E-Physics and them using the calculations from Appendix A changed the heat generated by the coil according to the coil current. As the current density within the coil increases as does the heat generated and thus the temperature of the housing.

Appendix C: Materials

Part	Material	Magnetic Properties	Thermal Properties		Electrical Properties	Density (kg/m^3)
		Curie Temperature (°C)	Thermal Conductivity (W/m*K)	CTE (µm/m*°C)	Electrical Resistivity (Ω*m)	
Housing	Steel 1045	1043	51.9	13.15	1.62E-07	7870
Stators						
Rod						
Coil	Cu	-	385	20.6	1.70E-08	8960
Magnets	NdFeB	310	2.931	3.4	0.00016	7650
Rotor	Polyetherimide	-	0.376	55.6	1.98E+14	1315

Appendix D: Diagrams

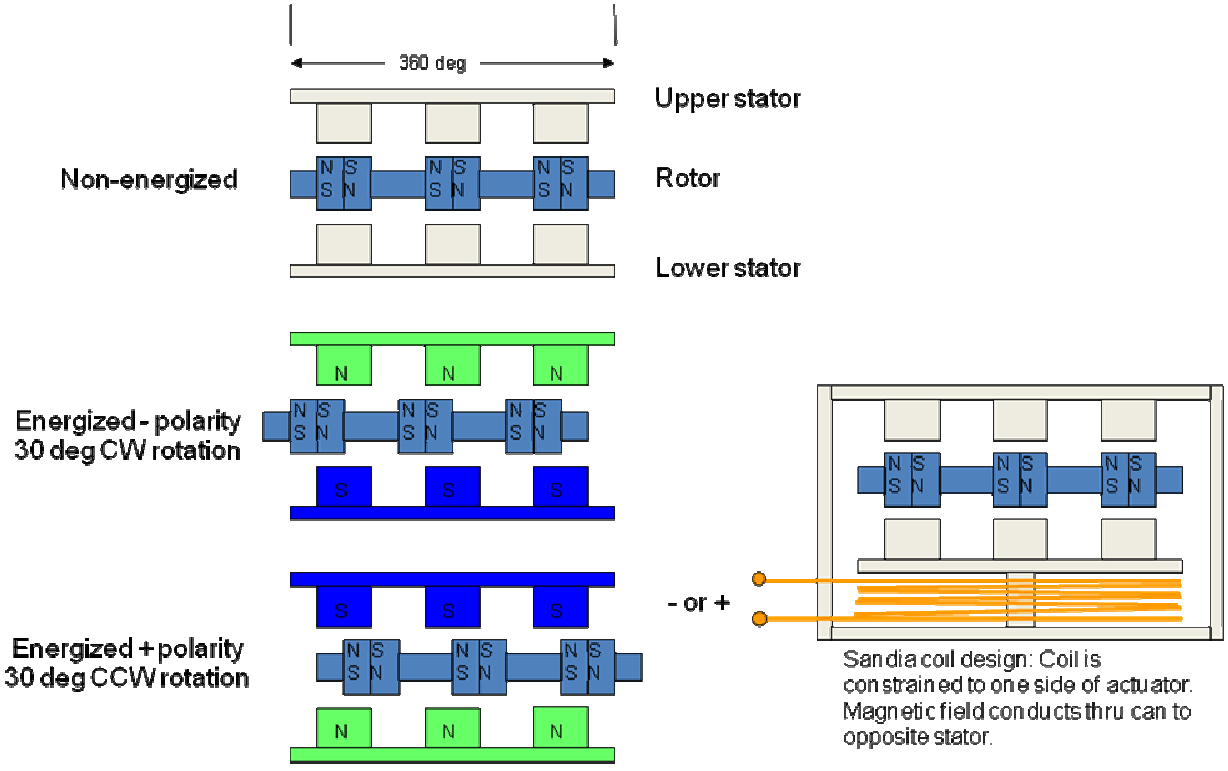

The diagram above illustrates the operation of our final design. When the actuator is not energized, the rotor is in a neutral position. Depending on what polarity the stator is magnetized in, the rotor will move to a new position.

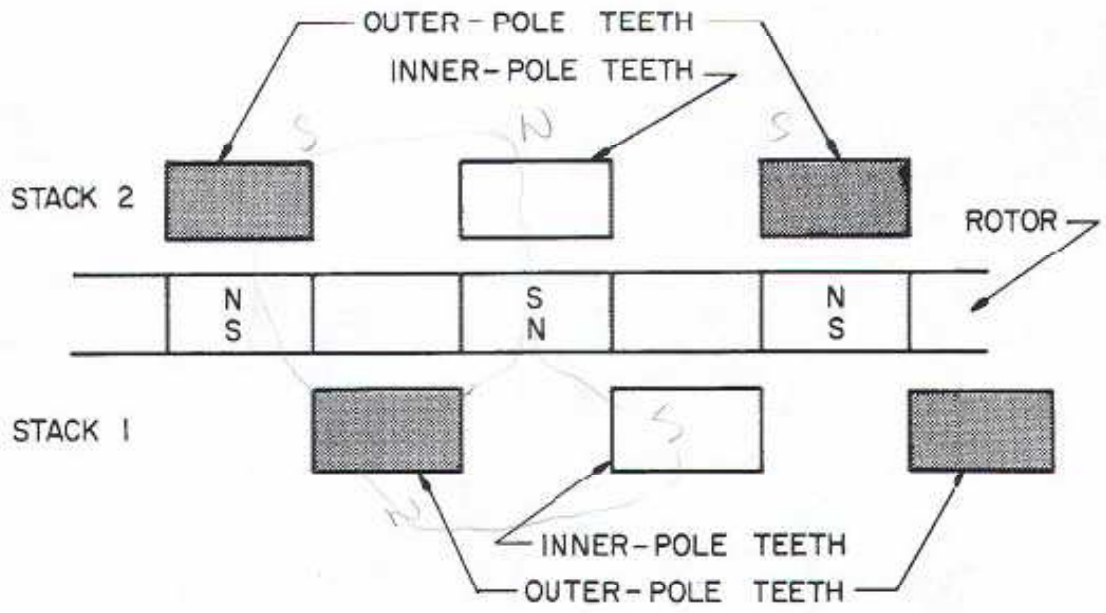

Figure 3. Inner-pole, outer-pole, and rotor relation.

The above diagram shows the operation of a single coil, two-stator actuator. Its shows the same operational principles as the above diagram, which corresponds to our final design.

Appendix E: Solidworks Drawings

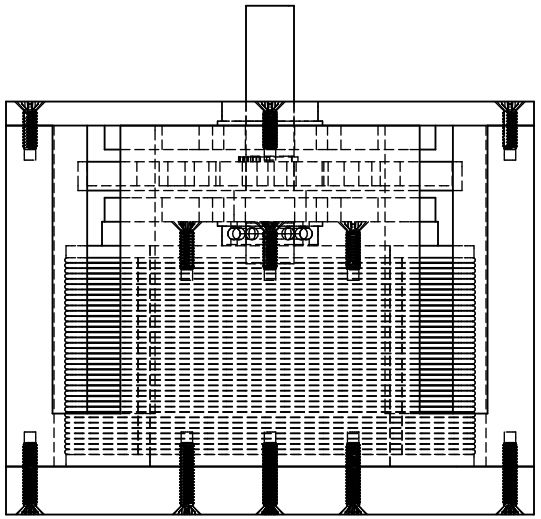

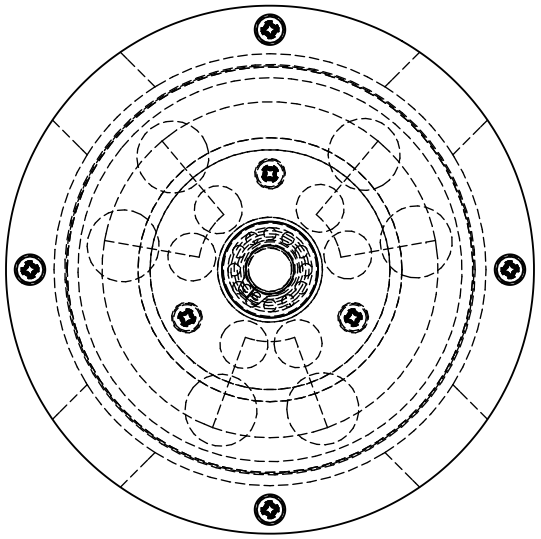

		UNLESS OTHERWISE SPECIFIED:		NAME	DATE
		DIMENSIONS ARE IN INCHES	DRAWN	RBHOOGE	3/30/2008
			CHECKED		
			ENG APPR.		
			MFG APPR.		
			Q.A.		
			COMMENTS:		
		MATERIAL N/A			
NEXT ASSY	USED ON	FINISH N/A			
APPLICATION					

TITLE:

TOP LEVEL VIEW

SIZE	DWG. NO.	REV
A	N/A	
SCALE: 1:1	WEIGHT:	SHEET 1 OF 17

PROPRIETARY AND CONFIDENTIAL

THE INFORMATION CONTAINED IN THIS DRAWING IS THE SOLE PROPERTY OF SANDIA NATIONAL LABS. ANY REPRODUCTION IN PART OR AS A WHOLE WITHOUT THE WRITTEN PERMISSION OF SANDIA NATIONAL LABS IS PROHIBITED.

5 4 3 2 1

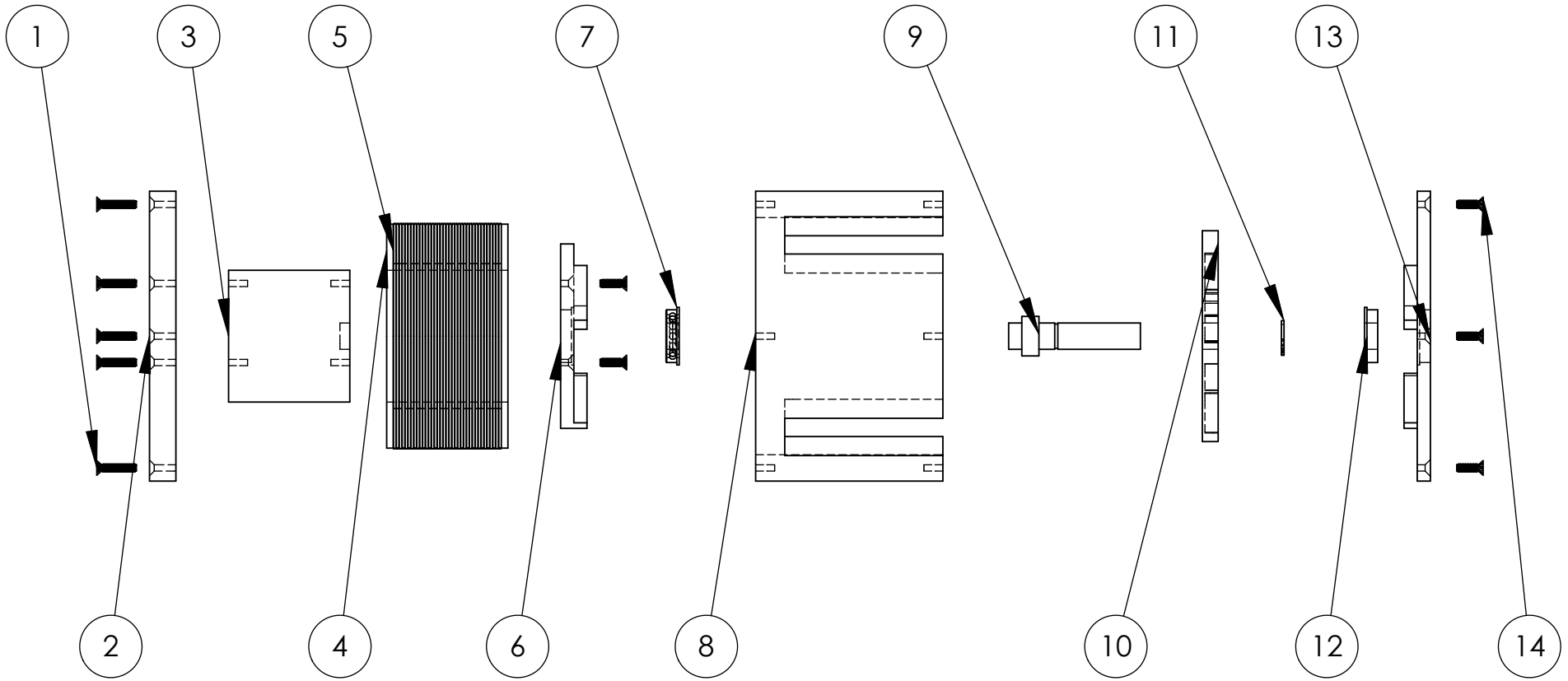

		UNLESS OTHERWISE SPECIFIED:		NAME	DATE
		DIMENSIONS ARE IN INCHES	DRAWN	RBHOOGE	3/30/2008
			CHECKED		
			ENG APPR.		
			MFG APPR.		
			Q.A.		
			COMMENTS:		
		MATERIAL N/A			
NEXT ASSY	USED ON	FINISH N/A			
APPLICATION					

PROPRIETARY AND CONFIDENTIAL

THE INFORMATION CONTAINED IN THIS DRAWING IS THE SOLE PROPERTY OF SANDIA NATIONAL LABS. ANY REPRODUCTION IN PART OR AS A WHOLE WITHOUT THE WRITTEN PERMISSION OF SANDIA NATIONAL LABS IS PROHIBITED.

TITLE:

EXPLODED VIEW

SIZE	DWG. NO.	REV
A	N/A	
SCALE: 1:1.5	WEIGHT:	SHEET 2 OF 17

5 4 3 2 1

PART NUMBER	PART NAME	MATERIAL	QTY.
1	Flat Head 0.375	STAINLESS STEEL	7
2	Base Plate	1045 MEDIUM-CARBON STEEL	1
3	Coil Core	1045 MEDIUM-CARBON STEEL	1
4	Spool	POLYETHERMIDE	1
5	Coil	22 GAUGE COPPER WIRE	1
6	Lower Stator	1045 MEDIUM-CARBON STEEL	1
7	Ball Bearing	STAINLESS STEEL	1
8	Housing	1045 MEDIUM-CARBON STEEL	1
9	shaft	ALUMINUM 6061	1
10	Rotor	ALUMINUM 6061	1
11	Snap Ring	STAINLESS STEEL	1
12	Bushing	BRASS	1
13	Upper Stator	1045 MEDIUM-CARBON STEEL	1
14	Flat Head 0.25	STAINLESS STEEL	7

PROPRIETARY AND CONFIDENTIAL

THE INFORMATION CONTAINED IN THIS DRAWING IS THE SOLE PROPERTY OF SANDIA NATIONAL LABS. ANY REPRODUCTION IN PART OR AS A WHOLE WITHOUT THE WRITTEN PERMISSION OF SANDIA NATIONAL LABSIS PROHIBITED.

		UNLESS OTHERWISE SPECIFIED:		NAME	DATE
		DIMENSIONS ARE IN INCHES	DRAWN	RBHOOGE	3/30/2008
			CHECKED		
			ENG APPR.		
			MFG APPR.		
			Q.A.		
			COMMENTS:		
		MATERIAL N/A			
NEXT ASSY	USED ON	FINISH N/A			
APPLICATION					

TITLE:

BILL OF MATERIALS

SIZE	DWG. NO.	REV
A	N/A	

SCALE: 1:1 | WEIGHT: | SHEET 3 OF 17

5 4 3 2 1

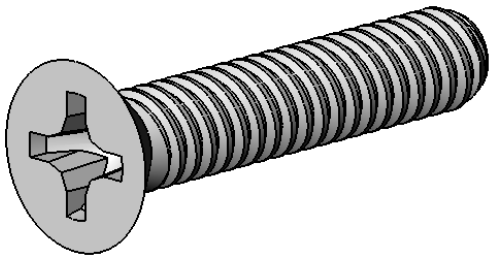

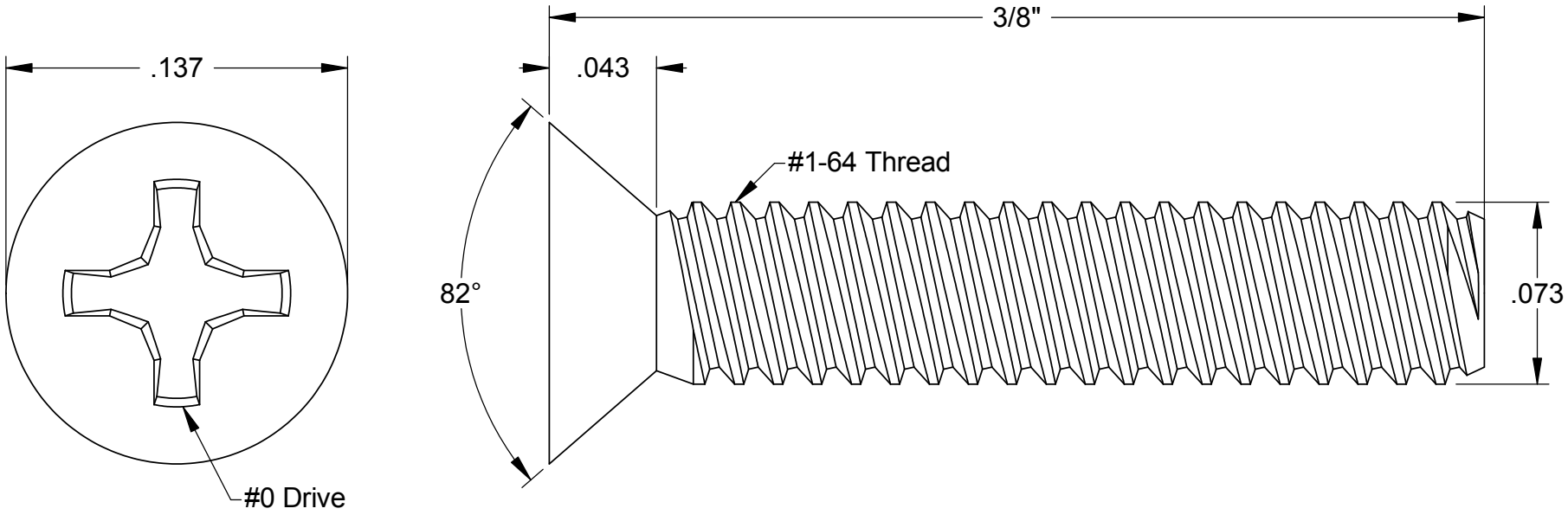

McMASTER-CARR CAD	PART NUMBER **91771A068**
http://www.mcmaster.com © 2005 McMaster-Carr Supply Company	18-8 Stainless Steel Phillips Flat Head Machine Screw

Unless otherwise specified, dimensions are in inches. Information in this drawing is provided for reference only.

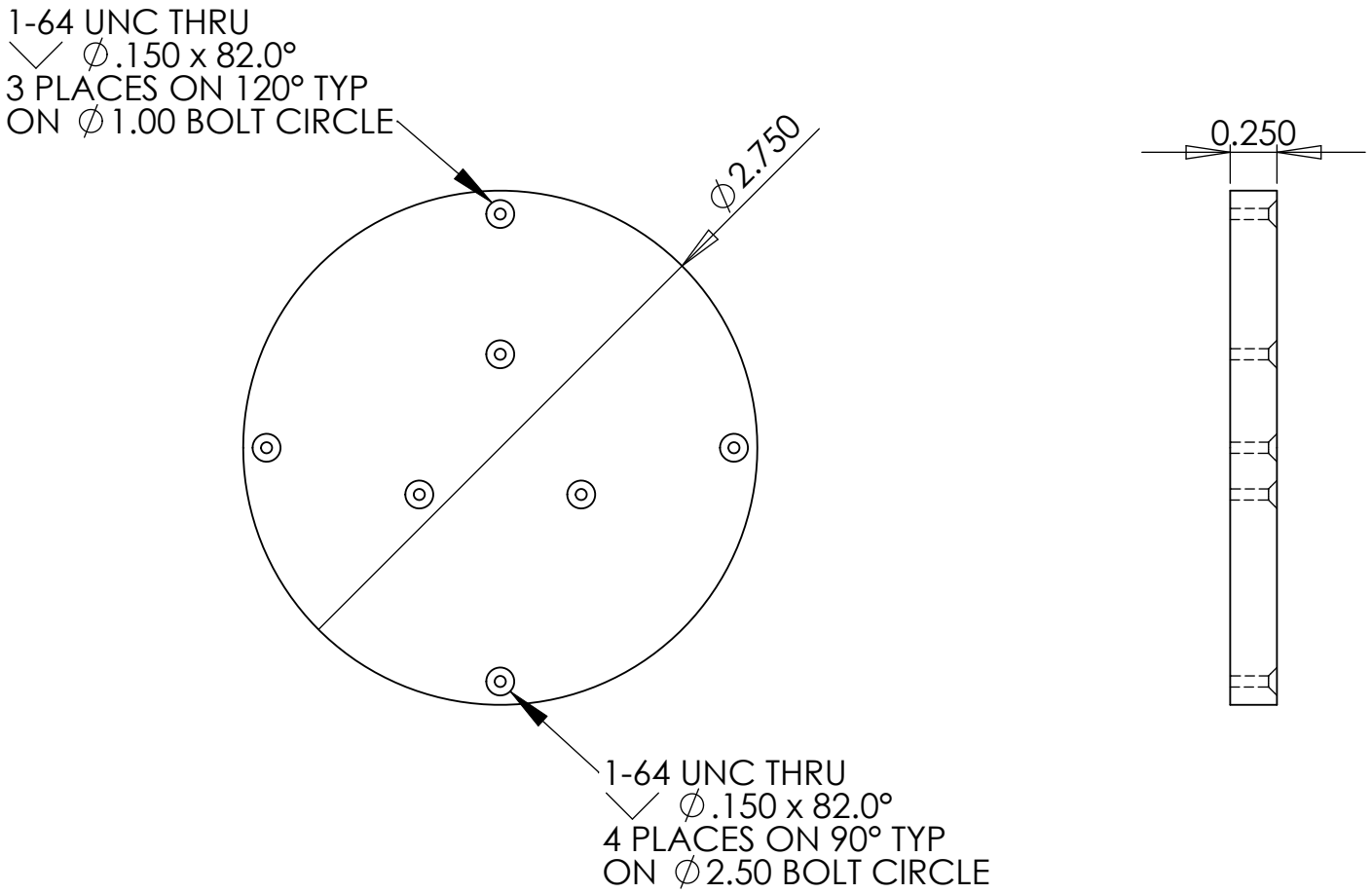

		UNLESS OTHERWISE SPECIFIED:		NAME	DATE
		DIMENSIONS ARE IN INCHES	DRAWN	RBHOOGE	3/30/2008
			CHECKED		
			ENG APPR.		
			MFG APPR.		
			Q.A.		
			COMMENTS:		
		MATERIAL 1045 MEDIUM-CARBON STEEL			
NEXT ASSY	USED ON	FINISH N/A			
APPLICATION					

TITLE:

BASE PLATE

SIZE	DWG. NO.	REV
A	2	

SCALE: 1:1 | WEIGHT: | SHEET 5 OF 17

PROPRIETARY AND CONFIDENTIAL

THE INFORMATION CONTAINED IN THIS DRAWING IS THE SOLE PROPERTY OF SANDIA NATIONAL LABS. ANY REPRODUCTION IN PART OR AS A WHOLE WITHOUT THE WRITTEN PERMISSION OF SANDIA NATIONAL LABS IS PROHIBITED.

5 4 3 2 1

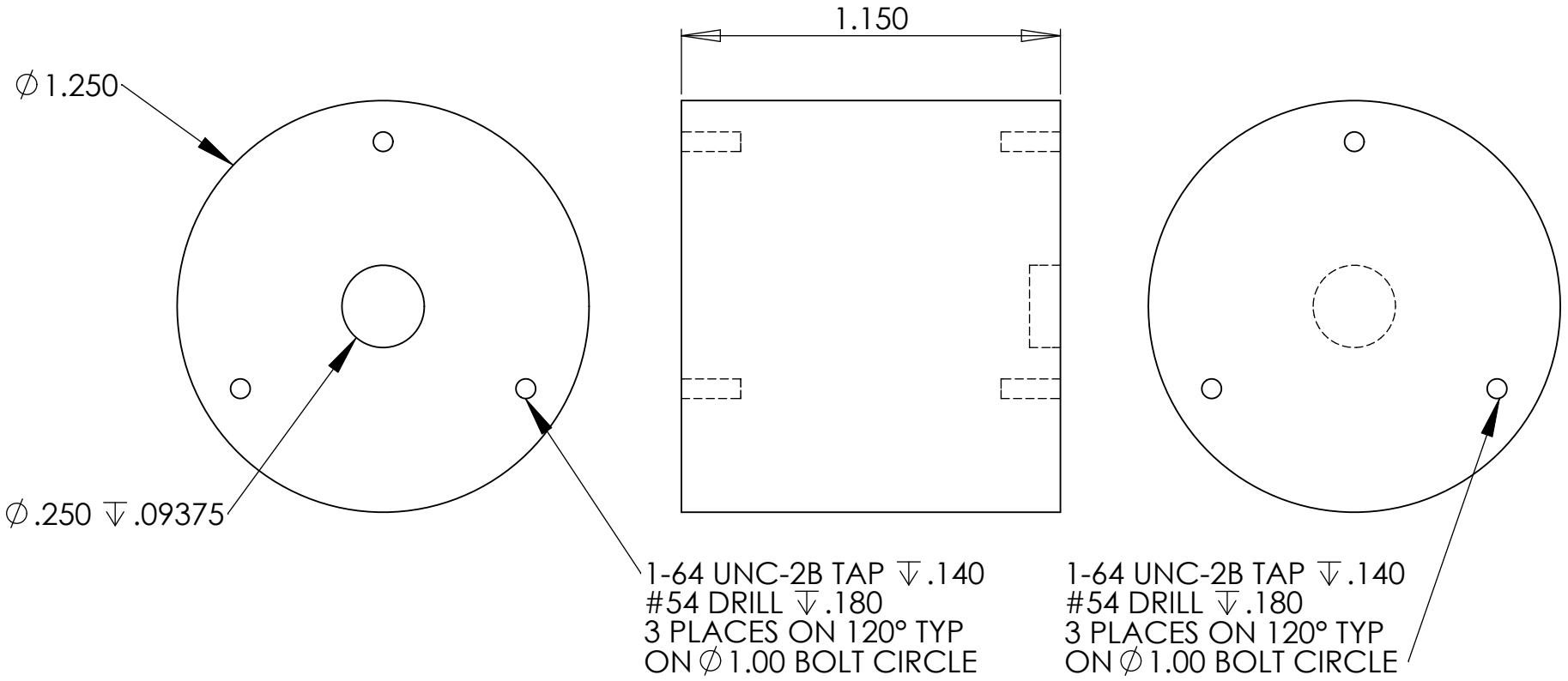

PROPRIETARY AND CONFIDENTIAL

THE INFORMATION CONTAINED IN THIS DRAWING IS THE SOLE PROPERTY OF SANDIA NATIONAL LABS. ANY REPRODUCTION IN PART OR AS A WHOLE WITHOUT THE WRITTEN PERMISSION OF SANDIA NATIONAL LABS IS PROHIBITED.

NEXT ASSY	USED ON	
APPLICATION		

UNLESS OTHERWISE SPECIFIED:

DIMENSIONS ARE IN INCHES

MATERIAL
1045 MEDIUM-CARBON STEEL

FINISH
N/A

	NAME	DATE
DRAWN	RBHOOGE	3/30/2008
CHECKED		
ENG APPR.		
MFG APPR.		
Q.A.		

COMMENTS:

TITLE:

COIL CORE

SIZE	DWG. NO.	REV
A	3	

SCALE: 2:1	WEIGHT:	SHEET 6 OF 17

5 4 3 2 1

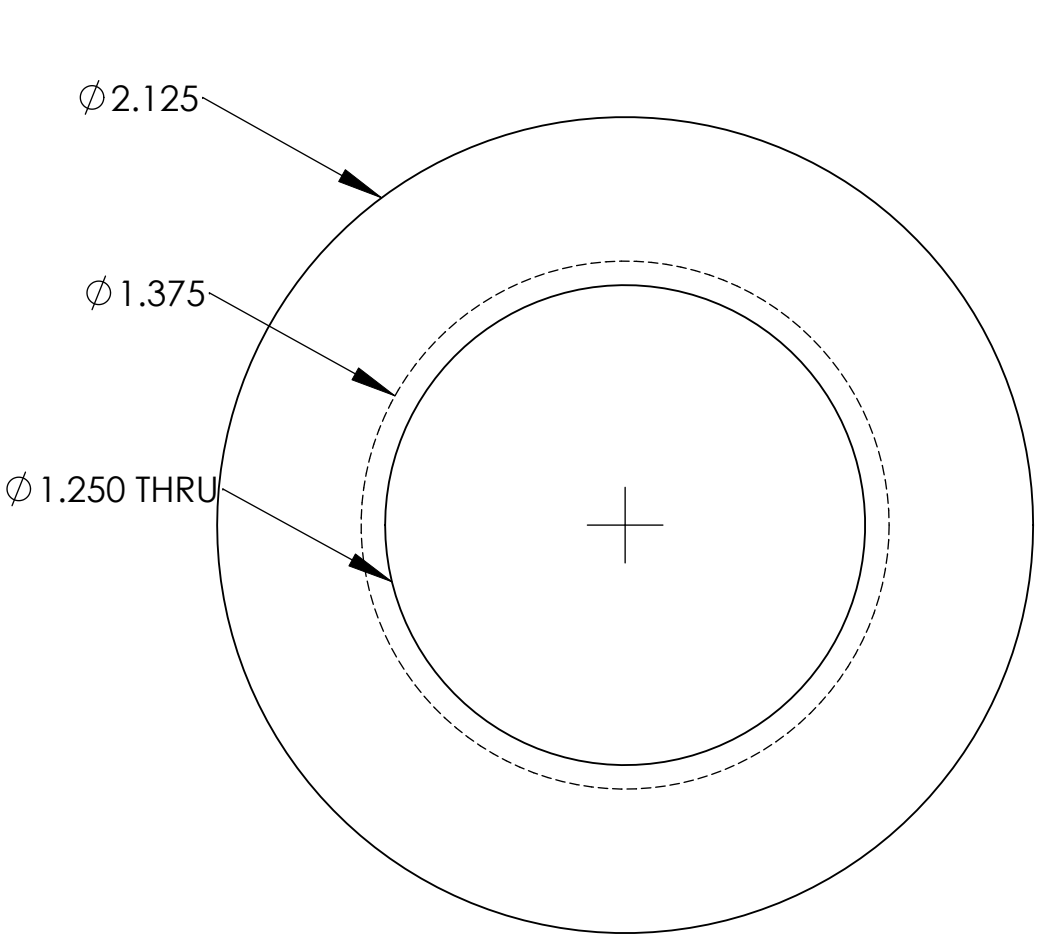

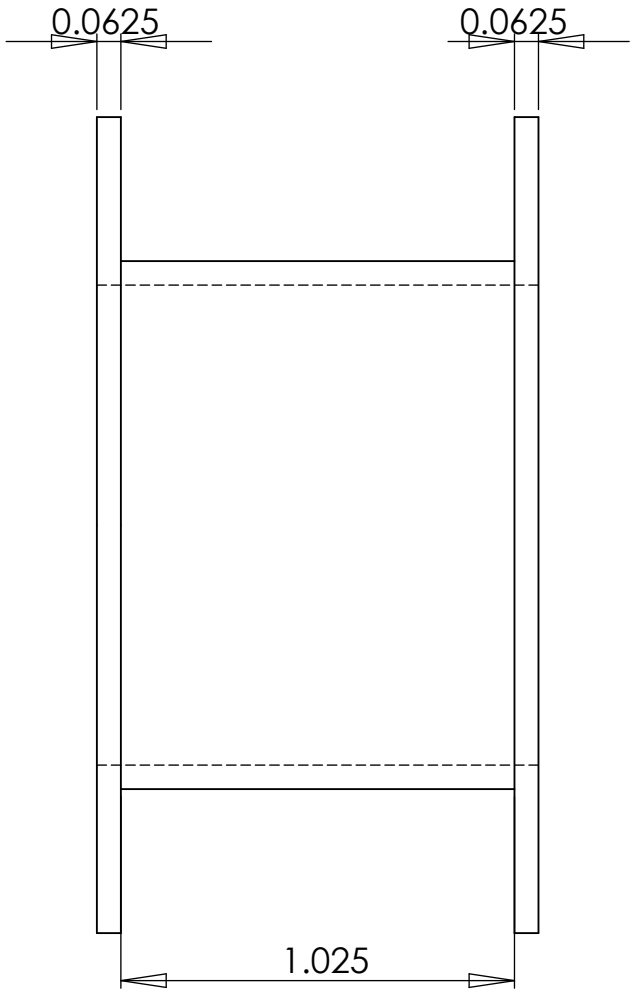

		UNLESS OTHERWISE SPECIFIED:		NAME	DATE
		DIMENSIONS ARE IN INCHES	DRAWN	RBHOOGE	3/30/2008
			CHECKED		
			ENG APPR.		
			MFG APPR.		
			Q.A.		
			COMMENTS:		
		MATERIAL POLYETHERIMIDE			
NEXT ASSY	USED ON	FINISH N/A			
APPLICATION					

PROPRIETARY AND CONFIDENTIAL

THE INFORMATION CONTAINED IN THIS DRAWING IS THE SOLE PROPERTY OF SANDIA NATIONAL LABS. ANY REPRODUCTION IN PART OR AS A WHOLE WITHOUT THE WRITTEN PERMISSION OF SANDIA NATIONAL LABS IS PROHIBITED.

TITLE:

SPOOL

SIZE	DWG. NO.	REV
A	4	
SCALE: 2:1	WEIGHT:	SHEET 7 OF 17

5 4 3 2 1

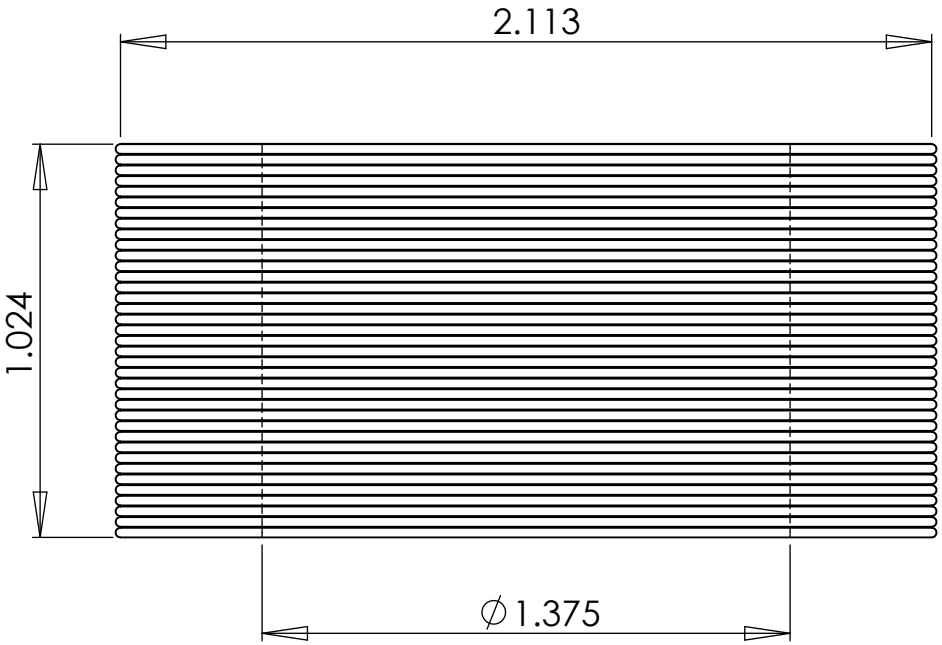

		UNLESS OTHERWISE SPECIFIED:		NAME	DATE
		DIMENSIONS ARE IN INCHES	DRAWN	RBHOOGE	3/30/2008
			CHECKED		
			ENG APPR.		
			MFG APPR.		
			Q.A.		
			COMMENTS:		
		MATERIAL 22 GAUGE COPPER WIRE			
NEXT ASSY	USED ON	FINISH N/A			
APPLICATION					

PROPRIETARY AND CONFIDENTIAL

THE INFORMATION CONTAINED IN THIS DRAWING IS THE SOLE PROPERTY OF SANDIA NATIONAL LABS. ANY REPRODUCTION IN PART OR AS A WHOLE WITHOUT THE WRITTEN PERMISSION OF SANDIA NATIONAL LABS IS PROHIBITED.

TITLE:

COIL

SIZE	DWG. NO.	REV
A	5	

SCALE: 2:1	WEIGHT:	SHEET 8 OF 17

5 4 3 2 1

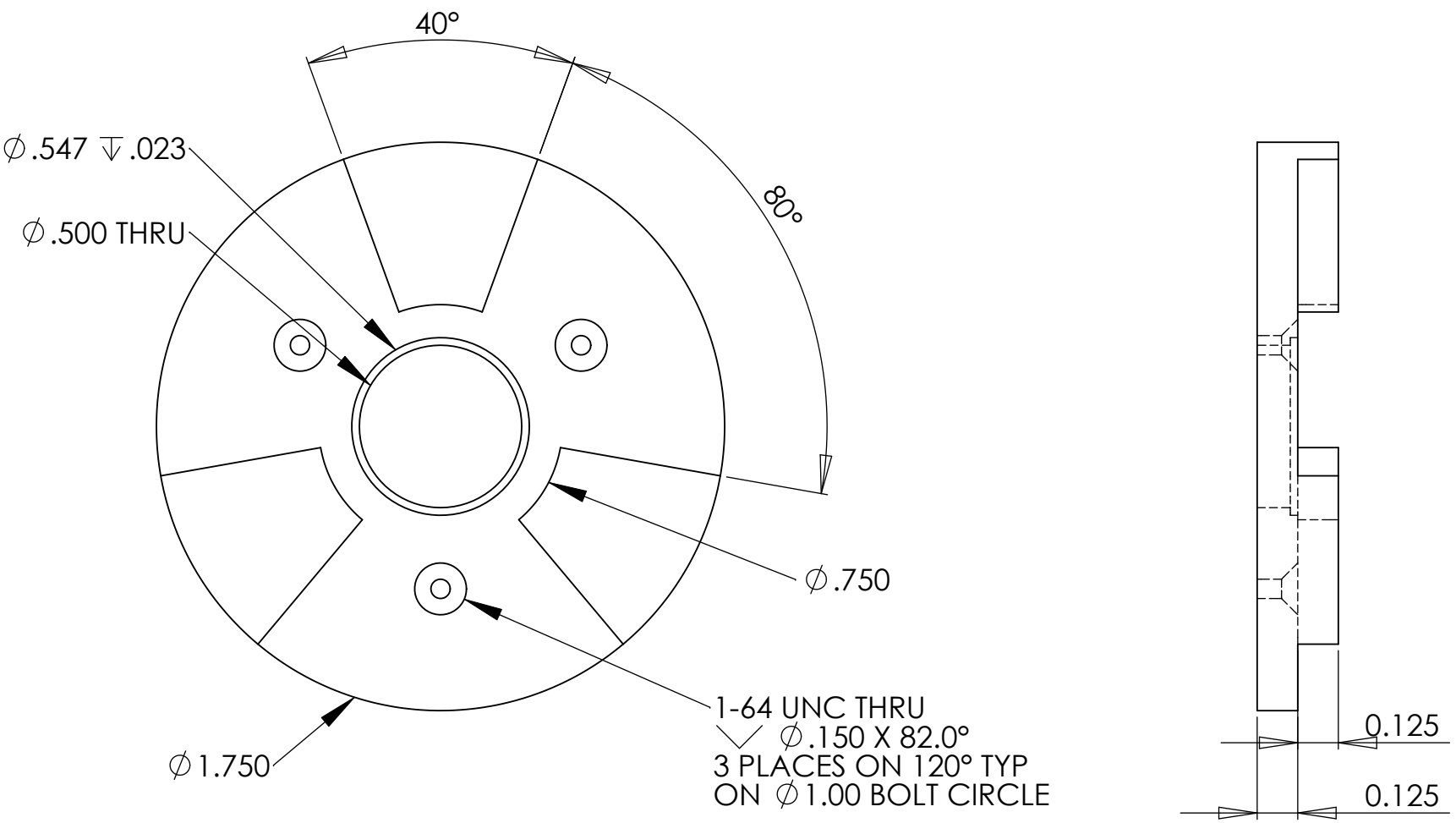

		UNLESS OTHERWISE SPECIFIED:		NAME	DATE
		DIMENSIONS ARE IN INCHES	DRAWN	RBHOOGE	3/30/2008
			CHECKED		
			ENG APPR.		
			MFG APPR.		
			Q.A.		
			COMMENTS:		
		MATERIAL 1045 MEDIUM-CARBON STEEL			
NEXT ASSY	USED ON	FINISH N/A			
APPLICATION					

TITLE:

LOWER STATOR

SIZE	DWG. NO.	REV
A	6	

SCALE: 2:1 | WEIGHT: | SHEET 9 OF 17

PROPRIETARY AND CONFIDENTIAL

THE INFORMATION CONTAINED IN THIS DRAWING IS THE SOLE PROPERTY OF SANDIA NATIONAL LABS. ANY REPRODUCTION IN PART OR AS A WHOLE WITHOUT THE WRITTEN PERMISSION OF SANDIA NATIONAL LABS IS PROHIBITED.

5 4 3 2 1

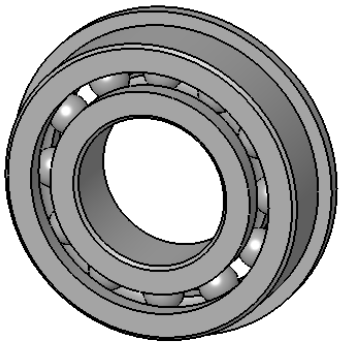

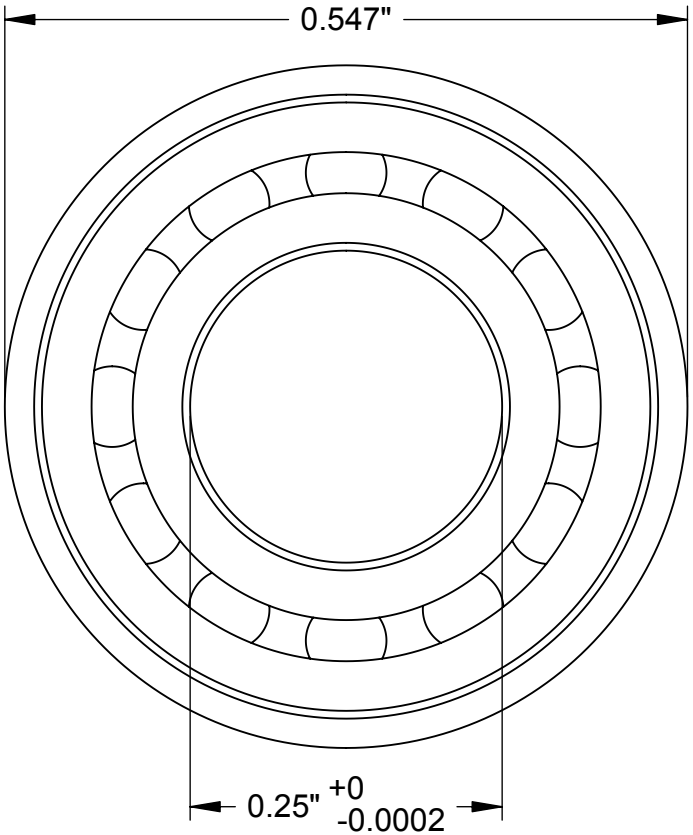

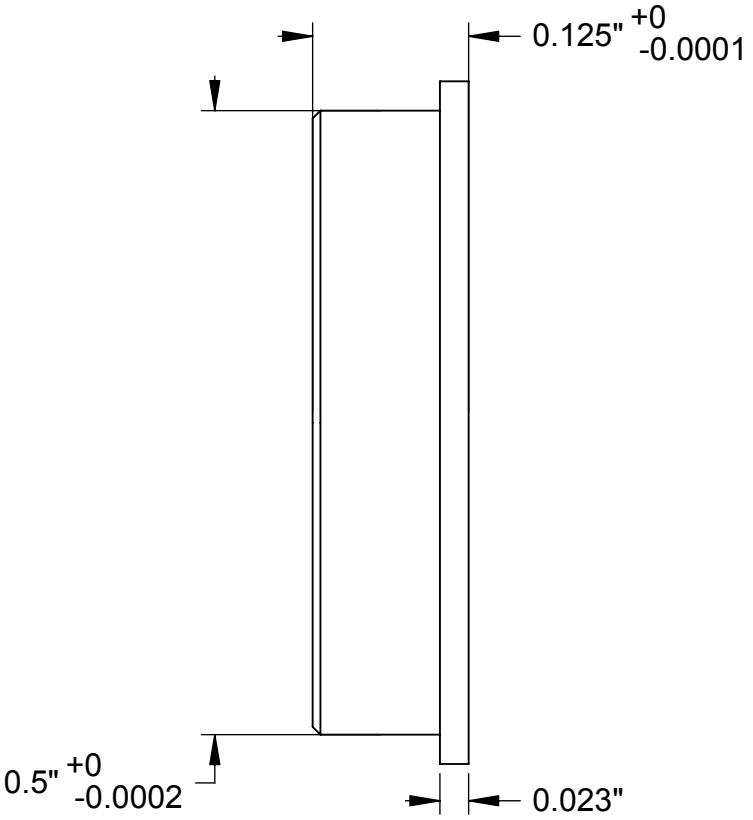

McMASTER-CARR CAD

PART NUMBER **4259T15**

http://www.mcmaster.com

© 2007 McMaster-Carr Supply Company

Type 440C Stainless Steel
Flanged Open Ball Bearing

Unless otherwise specified, dimensions are in inches. Information in this drawing is provided for reference only.

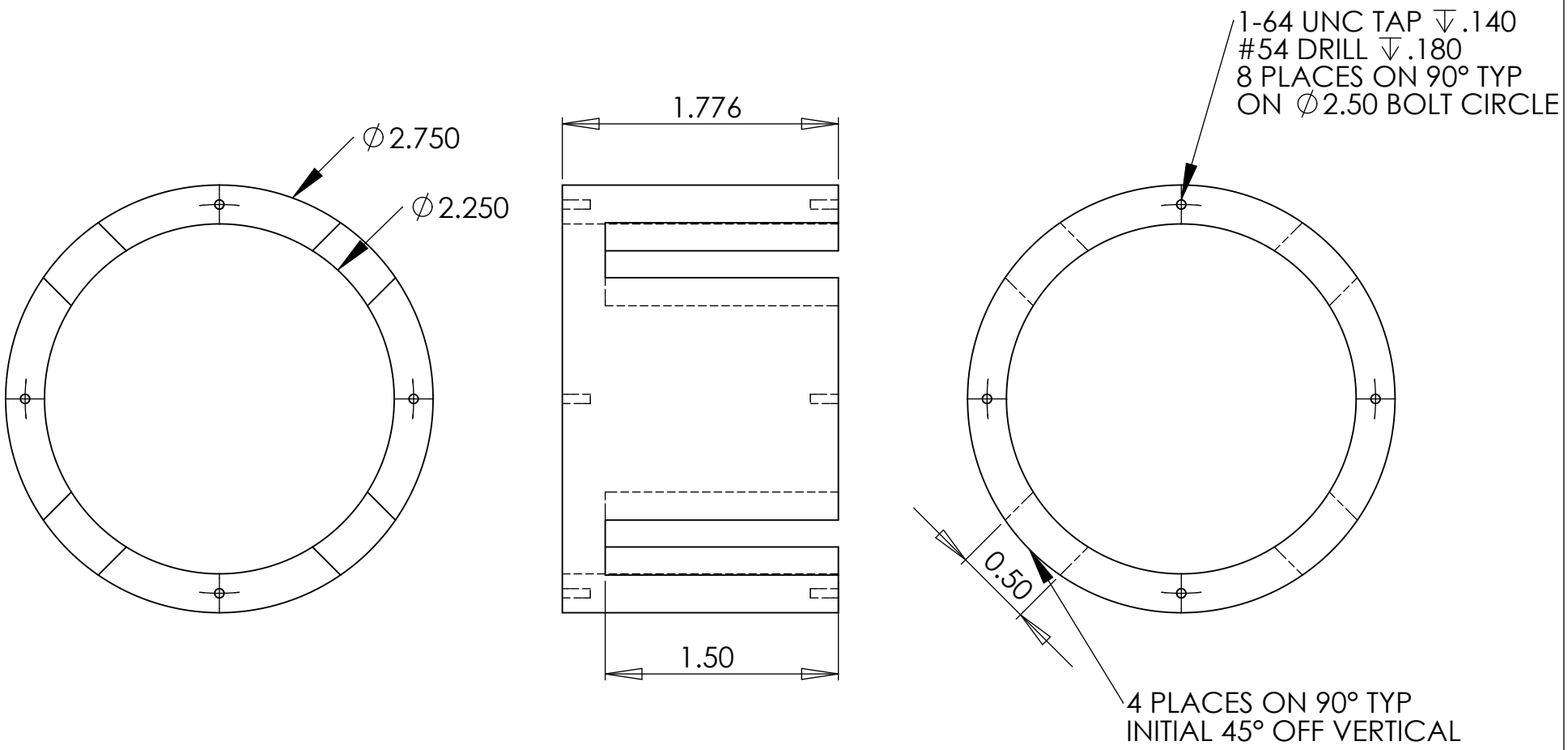

		UNLESS OTHERWISE SPECIFIED:		NAME	DATE
		DIMENSIONS ARE IN INCHES	DRAWN	RBHOOGE	3/30/2008
			CHECKED		
			ENG APPR.		
			MFG APPR.		
			Q.A.		
		MATERIAL 1045 MEDIUM-CARBON STEEL	COMMENTS:		
NEXT ASSY	USED ON	FINISH N/A			
APPLICATION					

TITLE:

HOUSING

SIZE	DWG. NO.	REV
A	8	
SCALE: 1:1	WEIGHT:	SHEET 11 OF 17

PROPRIETARY AND CONFIDENTIAL

THE INFORMATION CONTAINED IN THIS DRAWING IS THE SOLE PROPERTY OF SANDIA NATIONAL LABS. ANY REPRODUCTION IN PART OR AS A WHOLE WITHOUT THE WRITTEN PERMISSION OF SANDIA NATIONAL LABS IS PROHIBITED.

5 4 3 2 1

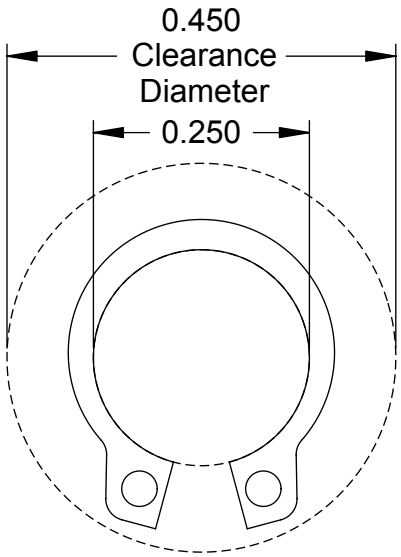

Expanded over Shaft

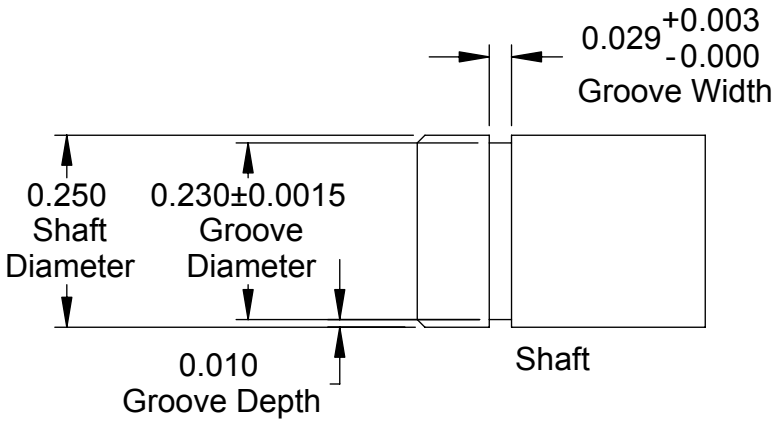

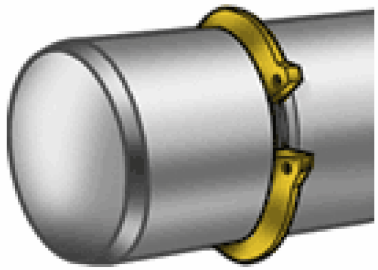

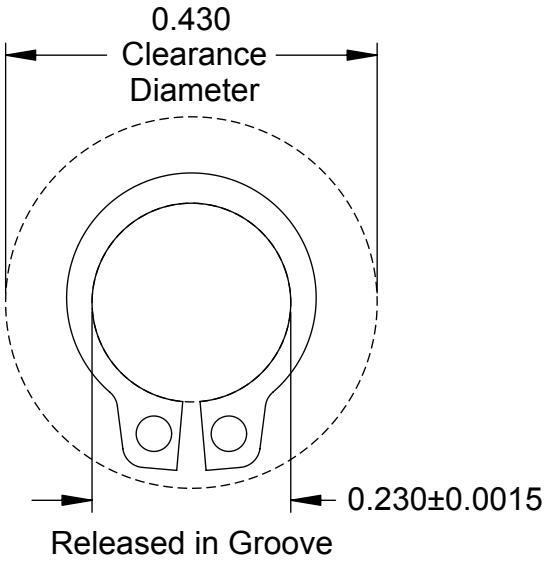

Released in Groove

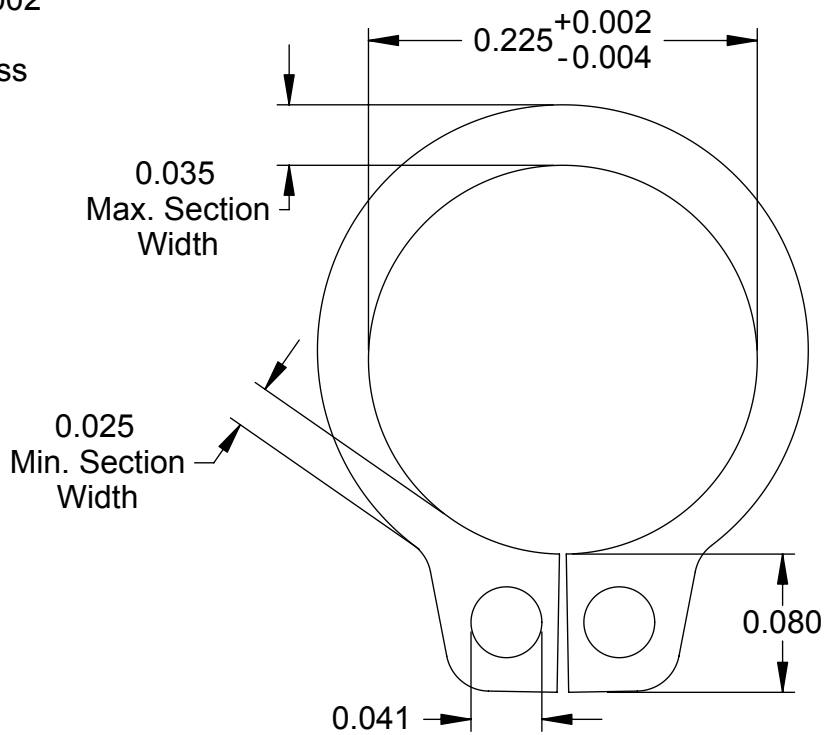

Note: Clearance diameter is the diameter of a housing that can pass freely over the ring.

McMASTER-CARR CAD	PART NUMBER **91590A113**
http://www.mcmaster.com © 2006 McMaster-Carr Supply Company	Stainless Steel External Retaining Ring
Unless otherwise specified, dimensions are in inches. Information in this drawing is provided for reference only.	

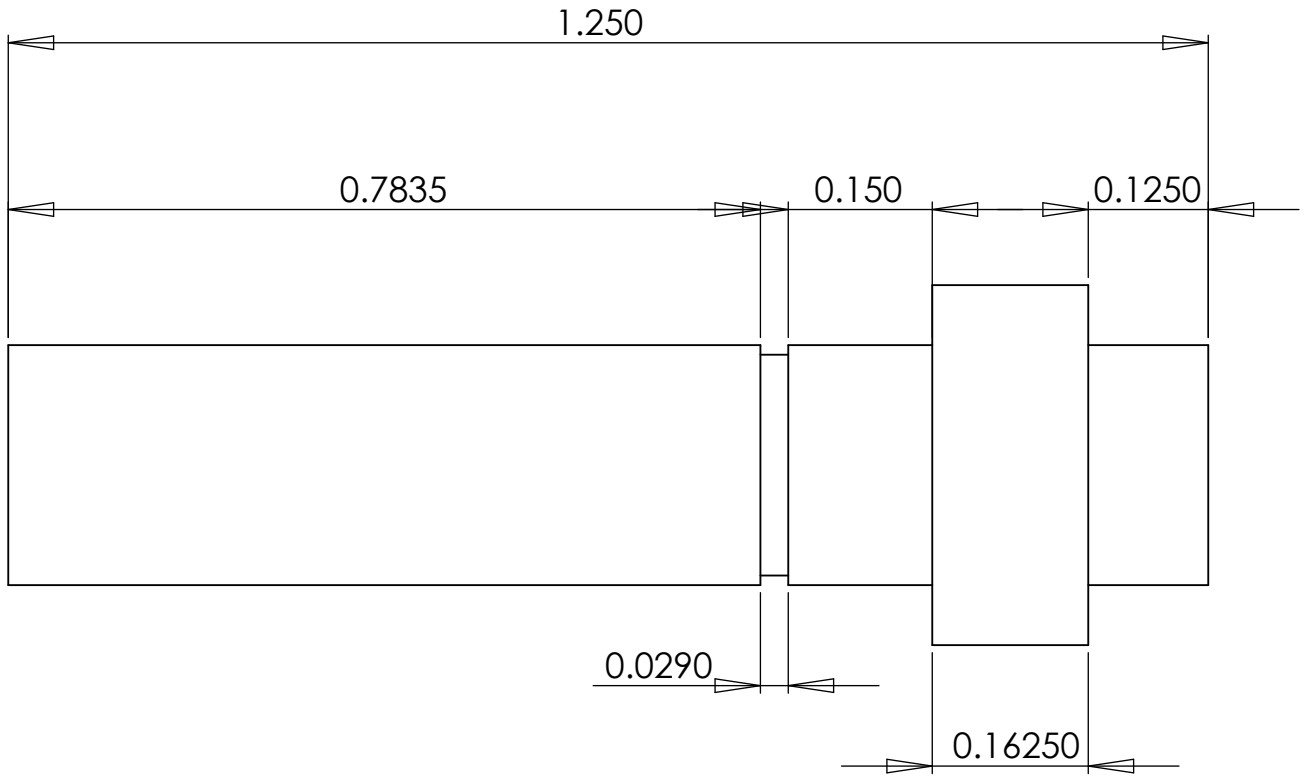

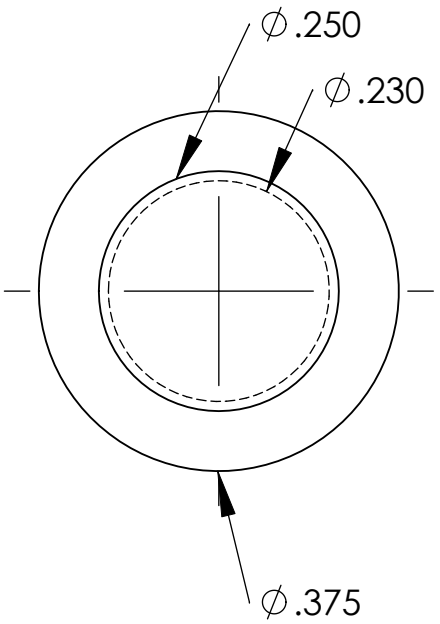

		UNLESS OTHERWISE SPECIFIED:		NAME	DATE
		DIMENSIONS ARE IN INCHES	DRAWN	RBHOOGE	3/30/2008
			CHECKED		
			ENG APPR.		
			MFG APPR.		
			Q.A.		
			COMMENTS:		
		MATERIAL ALUMINUM 6061			
NEXT ASSY	USED ON	FINISH N/A			
APPLICATION					

PROPRIETARY AND CONFIDENTIAL

THE INFORMATION CONTAINED IN THIS DRAWING IS THE SOLE PROPERTY OF SANDIA NATIONAL LABS. ANY REPRODUCTION IN PART OR AS A WHOLE WITHOUT THE WRITTEN PERMISSION OF SANDIA NATIONAL LABS IS PROHIBITED.

TITLE:

SHAFT

SIZE	DWG. NO.	REV
A	10	

SCALE: 2:1 | WEIGHT: | SHEET 13 OF 17

5 4 3 2 1

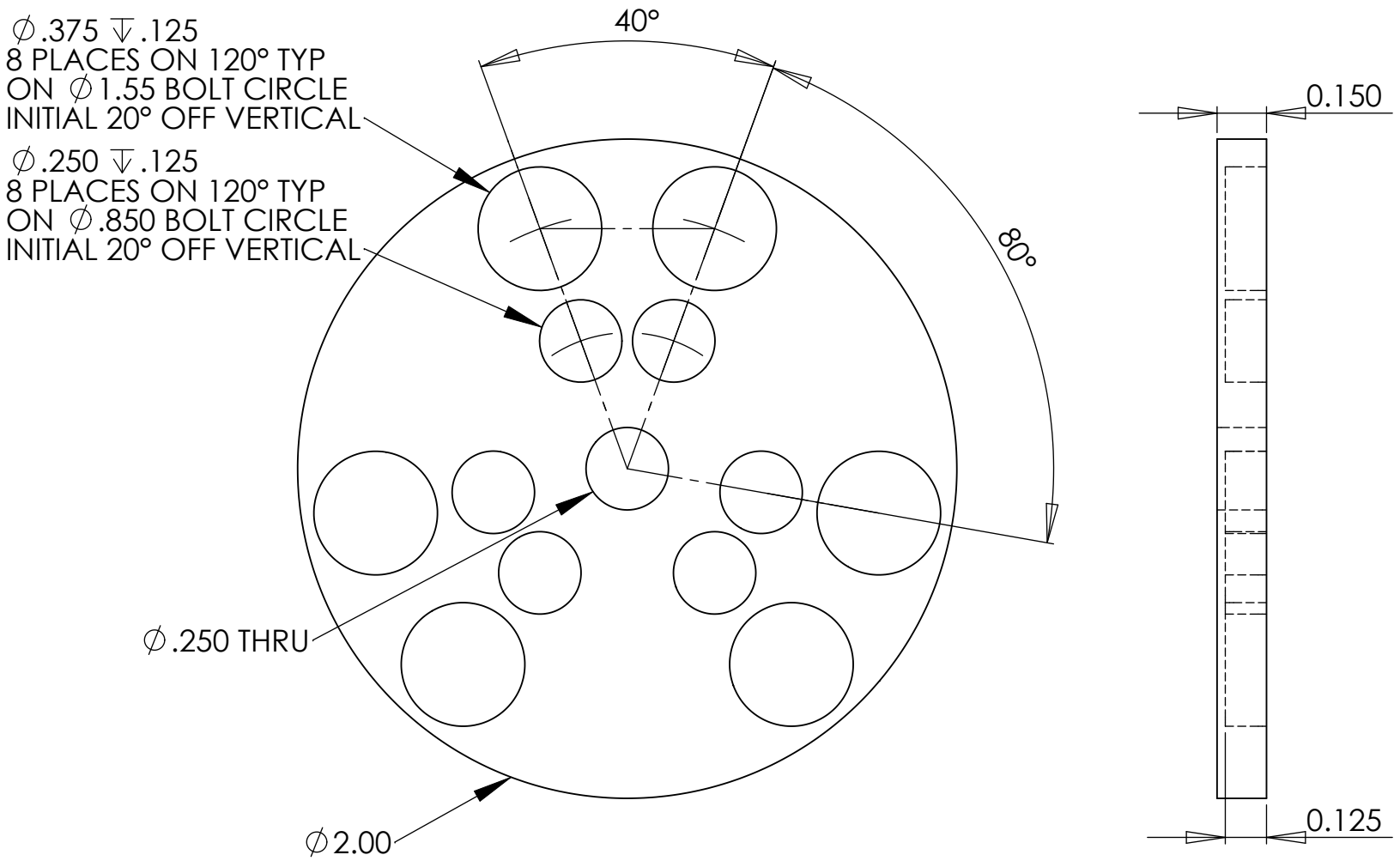

		UNLESS OTHERWISE SPECIFIED:		NAME	DATE
		DIMENSIONS ARE IN INCHES	DRAWN	RBHOOGE	3/30/2008
			CHECKED		
			ENG APPR.		
			MFG APPR.		
			Q.A.		
			COMMENTS:		
		MATERIAL ALUMINUM 6061			
NEXT ASSY	USED ON	FINISH N/A			
APPLICATION					

PROPRIETARY AND CONFIDENTIAL

THE INFORMATION CONTAINED IN THIS DRAWING IS THE SOLE PROPERTY OF SANDIA NATIONAL LABS. ANY REPRODUCTION IN PART OR AS A WHOLE WITHOUT THE WRITTEN PERMISSION OF SANDIA NATIONAL LABS IS PROHIBITED.

TITLE:

ROTOR

SIZE	DWG. NO.	REV
A	11	

SCALE: 2:1 | WEIGHT: | SHEET 14 OF 17

5 4 3 2 1

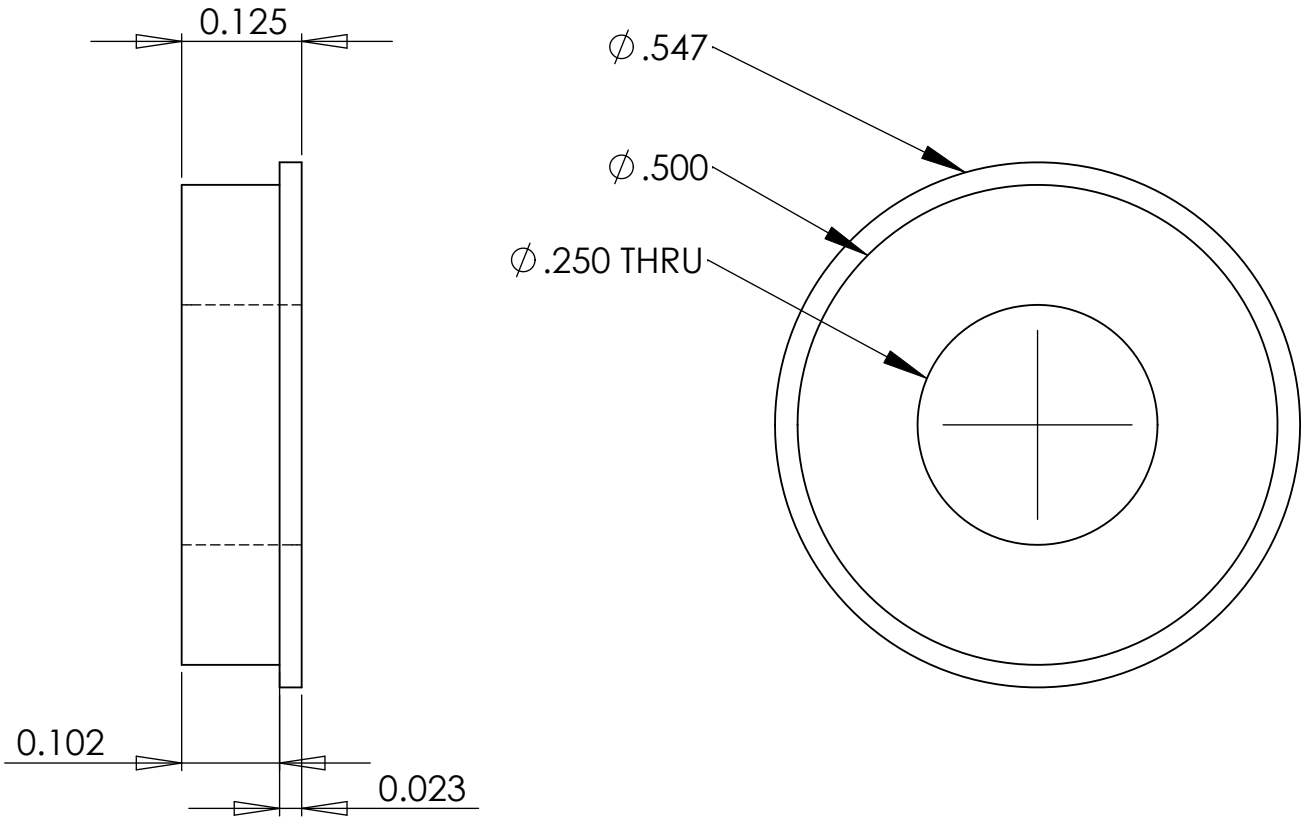

		UNLESS OTHERWISE SPECIFIED:		NAME	DATE
		DIMENSIONS ARE IN INCHES	DRAWN	RBHOOGE	3/30/2008
			CHECKED		
			ENG APPR.		
			MFG APPR.		
			Q.A.		
			COMMENTS:		
		MATERIAL BRASS			
NEXT ASSY	USED ON	FINISH			
APPLICATION					

PROPRIETARY AND CONFIDENTIAL

THE INFORMATION CONTAINED IN THIS DRAWING IS THE SOLE PROPERTY OF SANDIA NATIONAL LABS. ANY REPRODUCTION IN PART OR AS A WHOLE WITHOUT THE WRITTEN PERMISSION OF SANDIA NATIONAL LABS IS PROHIBITED.

TITLE:

BUSHING

SIZE	DWG. NO.	REV
A	12	

SCALE: 5:1 | WEIGHT: | SHEET 15 OF 17

5 4 3 2 1

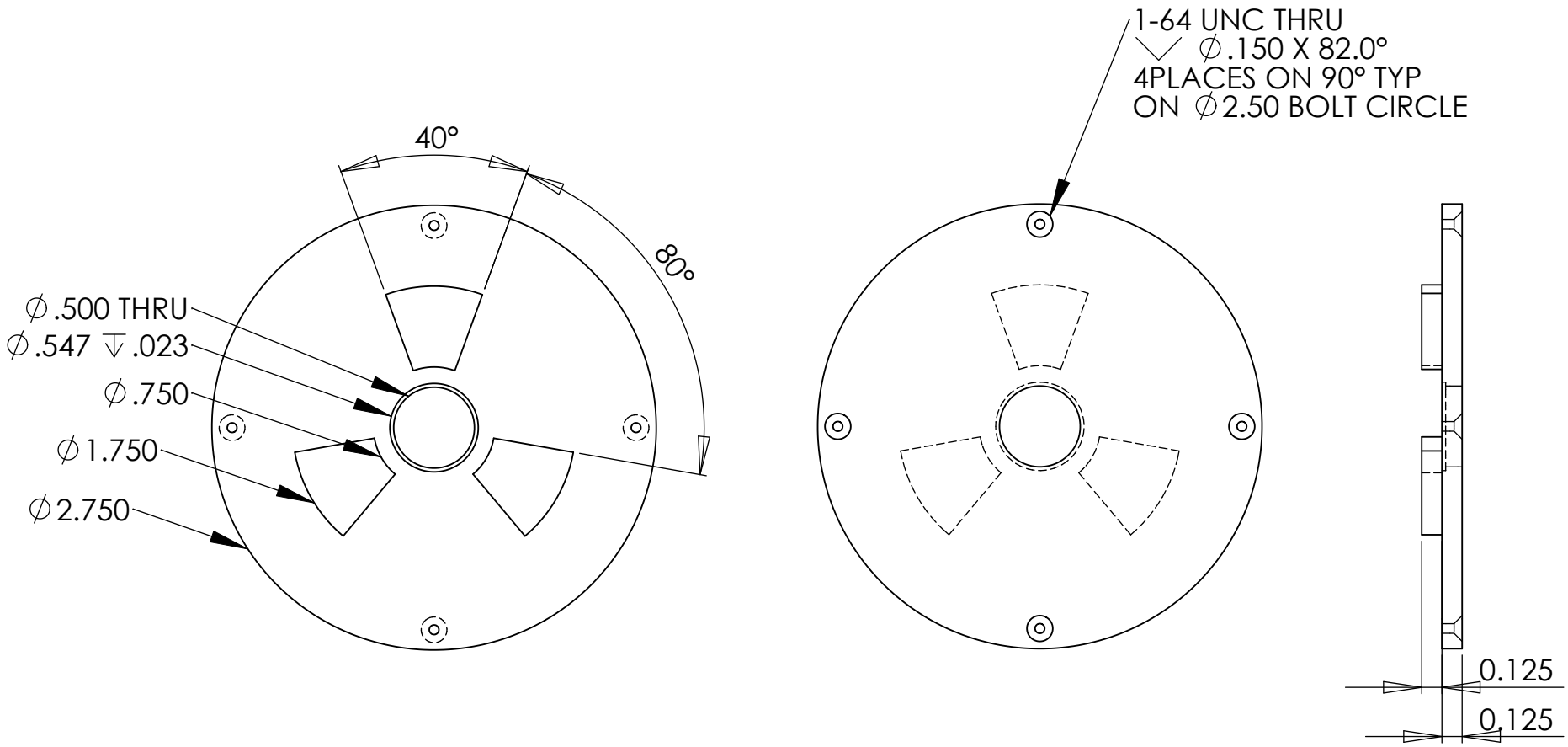

		UNLESS OTHERWISE SPECIFIED:		NAME	DATE
		DIMENSIONS ARE IN INCHES	DRAWN	RBHOOGE	3/30/2008
			CHECKED		
			ENG APPR.		
			MFG APPR.		
			Q.A.		
		MATERIAL 1045 MEDIUM-CARBON STEEL	COMMENTS:		
NEXT ASSY	USED ON	FINISH			
APPLICATION					

PROPRIETARY AND CONFIDENTIAL

THE INFORMATION CONTAINED IN THIS DRAWING IS THE SOLE PROPERTY OF SANDIA NATIONAL LABS. ANY REPRODUCTION IN PART OR AS A WHOLE WITHOUT THE WRITTEN PERMISSION OF SANDIA NATIONAL LABS IS PROHIBITED.

TITLE:

UPPER STATOR

SIZE	DWG. NO.	REV
A	13	

SCALE: 1:1 | WEIGHT: | SHEET 16 OF 17

5 4 3 2 1

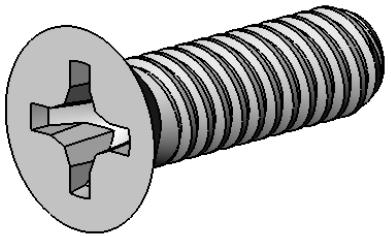

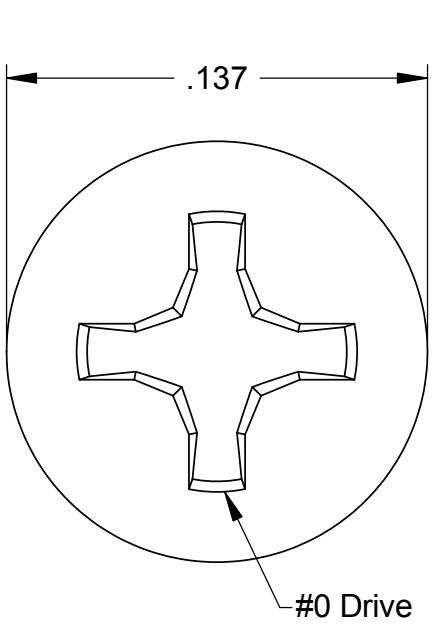

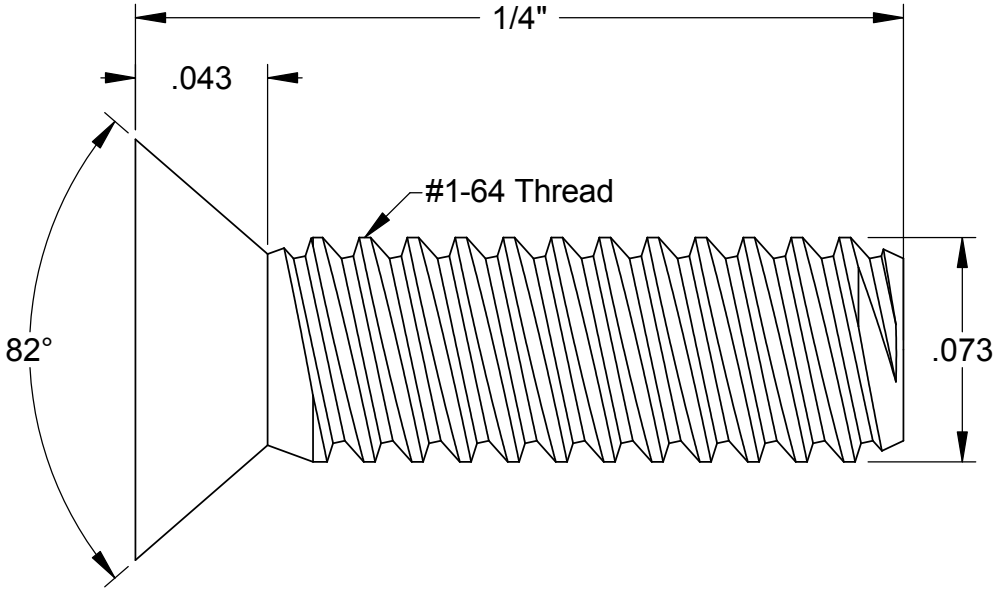

McMASTER-CARR CAD	PART NUMBER **91771A066**
http://www.mcmaster.com © 2005 McMaster-Carr Supply Company	18-8 Stainless Steel Phillips Flat Head Machine Screw

Unless otherwise specified, dimensions are in inches. Information in this drawing is provided for reference only.

Appendix F: Reference Papers

All rights reserved. No part of this book may be reproduced in any form or by any means without permission in writing.

© 1981 Incremental Motion Control Systems Society

Library of Congress Catalog Card No. 73-647018
ISBN 0-931538-03-3
ISSN 0092-1661

Published by the Incremental Motion Control Systems Society
Post Office Box 2772, Station A, Champaign, Illinois 61820

NOTICE: THIS MATERIAL MAY BE PROTECTED BY COPYRIGHT LAW (TITLE 17 U.S. CODE)

A DISK-ROTOR PERMANENT-MAGNET STEP MOTOR

B. C. Kuo

Department of Electrical Engineering
University of Illinois at Urbana-Champaign
Urbana, Illinois

W. H. Yeadon

Warner Electric Brake and Clutch Co.
Marengo, Illinois

I. INTRODUCTION

The canned type permanent-magnet (PM) step motors [1] have gained increased popularity commercially in recent years mainly due to their low cost, simplicity in construction, and light weight.

As the name implies, the housing of the canned-type PM step motor is a metal can. The stator teeth assemblies are punched out of metal sheets, and the stator windings are in the form of bobbin-wound coils. The rotor consists of a cylindrical piece of magnetic material which is magnetized with multiple numbers of poles with alternate polarities along the periphery of the rotor. Figure 1 shows the simplified cross-sectional views of the motor which has two stator sections. The teeth of one stator section are displaced from those of the other by one-half of a tooth pitch.

The stator coils are usually wound bifilar so that the motor can be driven by a unipolar driver as a four-phase motor, or, the bifilar windings can be so connected that the motor can be driven as a two-phase motor by a bipolar driver. Additional sections and phases can be added lengthwise to the motor to increase the torque output.

As shown in Figure 1, when one phase of the motor is energized, the magnetic flux is essentially confined to flow only within that section of the motor. Therefore, each section of the motor is essentially isolated from the other section(s) from a magnetic sense.

The purpose of this paper is to introduce a step motor that has a disk-shaped permanent-magnet rotor. The geometry, construction, principle of operation, and typical performance characteristics of the motor are presented. The analysis and computation of the magnetic circuits of the motor are given in another paper in these Proceedings.

The advantages of the disk-rotor PM motor are:

1. The motor diameter can be made smaller than a conventional cylindrical-rotor motor having similar performance characteristics.
2. Since the poles on the rotor are magnetized in the axial direction, oriented magnetic materials such as ceramic 5 or 8 may be used instead of the non-oriented materials such as ceramic 1, commonly used on cylindrical rotors with radial air gaps. The oriented material has a greater flux density which produces more torque per ampere of input current than a non-oriented material. As a result, the damping characteristics and the motor efficiency are improved.

II. CONSTRUCTION OF THE DISK-ROTOR MOTOR

Figure 2 shows the major components of the motor with four phases and a step resolution of 7.5 degrees (48 steps/revolution). As shown in Figure 2, the major components of the motor are:

a permanent-magnet rotor
two inner-pole assemblies
two outer-pole assemblies
two bobbin-wound coils
housing.

The two sets of inner-and outer-pole assemblies are positioned on opposite sides of the disk rotor. For the 48-step-per-revolution motor illustrated, the rotor is magnetized axially with 24 alternate North-South poles. There are 12 teeth on each of the inner- and outer-pole pieces. The tooth pitch of the inner-pole piece and the outer-pole piece is twice that of the rotor assembly. The relative positions of the inner-pole and the outer-pole assemblies on opposite sides of the rotor are offset by one-half of a tooth pitch. Figure 3 shows the relative positions between the rotor poles and the stator teeth of the two stacks. The two bobbin-wound coils can each be wound with a single winding

for bipolar driving, or with bifilar windings for unipolar driving.

As shown in Fig. 3, when the teeth of stack No. 1 of the stator are in alignment with the rotor poles, those of Stack No. 2 are in total misalignment. Thus, as the phase energization is switched from Stack 2 to Stack 1, the rotor will rotate one-half of a pole pitch of the rotor. The step angle of the motor is then given by

$$\theta_s = \frac{360}{2N_p} \text{ degrees} \qquad (1)$$

where N_p is the number of poles on one side of the PM rotor. For the case illustrated in Figure 1, there are 24 poles on the rotor, and θ_s is 7.5 deg/step, or the step resolution is 48 steps per revolution. N_p is also equal to the total number of teeth on the inner-pole piece and the outer-pole piece on one stack of the stator.

Figure 4 shows two simplified cross-sectional views of the disk-rotor motor for the purpose of illustrating the main flux paths. The main flux-carrying parts of the motor include the PM rotor, the inner poles, the outer poles, the hub, and the housing. The spacer, which is located at the center of the motor, is non-magnetic and divides the motor into two sections magnetically. The main flux path of the motor is described as shown in Figure 4. If we start at the surface of a North pole on stack No. 1 of the PM rotor, as shown in Figure 4, the magnetic flux will typically go through the following parts of the motor in succession:

1. North pole on the left side of the PM rotor
2. Main air gap
3. Inner pole
4. Hub
5. Air gap between hub and housing
6. Housing
7. Air gap between housing and outer pole
8. Outer pole
9. Main air gap
10. South pole on the left sice of the PM rotor, adjacent to the starting North pole.

The flux then traverses the depth of the rotor and exists at the North pole on the right side of the rotor, and then the same sequence as described above takes place in stack No. 2.

From Figure 4, we can see that one important difference between this disk-rotor motor and the conventional canned-type PM motor is that the flux paths of the former encompass the entire motor even when only one phase is excited, whereas the flux paths of the latter motor are confined to only the excited phase.

The coupling of both stacks of the motor by the magnetic flux also means that the torque develcped by the motor will be affected by the stator teeth on both sides of the rotor.

III. PERFORMANCE CHARACTERISTICS

The performance characteristics of a typical disk-rotor PM step motor are presented in this section. The physical dimensions of the motor are: length = 2 in., outer diameter = 2.5 in.

The electrical properties and characteristics are:

Number of phases:	4	(bifilar wound)
Winding resistance:	1.6	ohms per phase
Rated current:	1.75	Amp. per phase
Inductance:	11	mH (0 Amp. DC at detent position)

The single-step responses with one-phase-on and two-phase-on excitations are shown in Figures 5 and 6, respectively.

Figures 7 and 8 illustrate the static torque curves with one-phase-on and two-phase-on excitations measured under the stated conditions. Figure 9 gives the torque-speed curves of the motor.

IV. REFERENCES

[1] Heine, Guenther, "Small PM Stepping Motors as Dedicated Control Elements in Data Processing Technology," Proceedings of the Seventh Annual Symposium on Incremental Motion Control Systems and Devices, 1978, pp. 27-36.

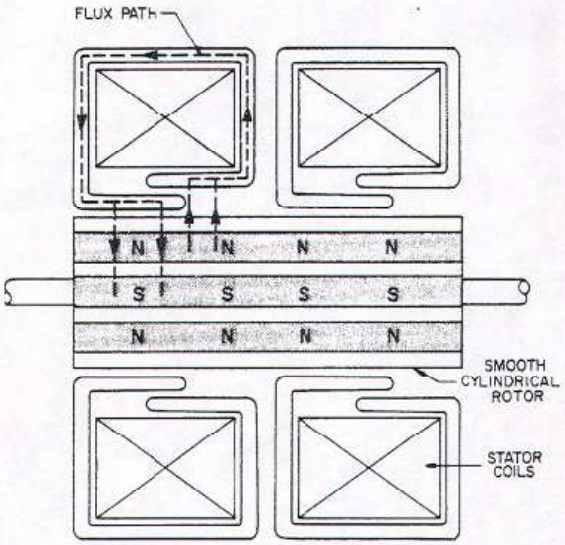

Figure 1. Cross-sectional view of the canned-type PM step motor.

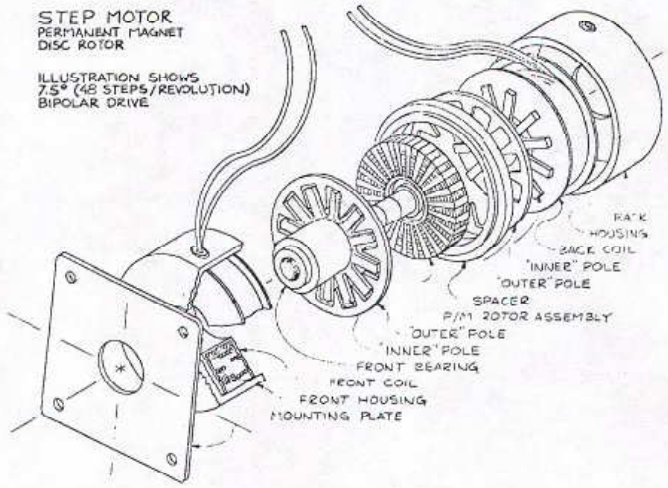

Figure 2. Principal components of the disk-rotor motor.

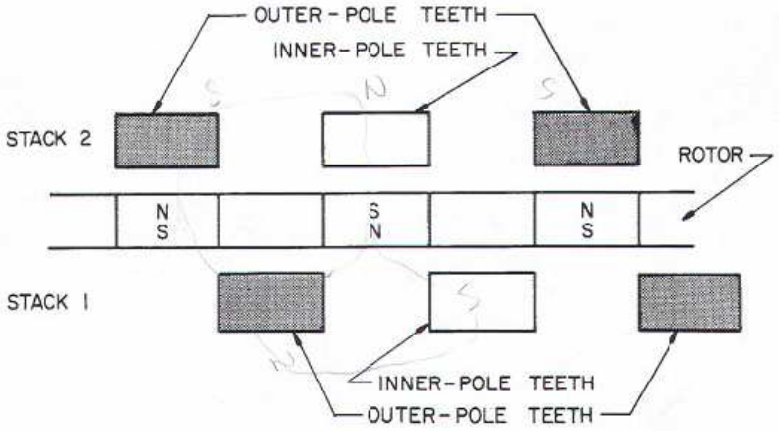

Figure 3. Inner-pole, outer-pole, and rotor relation.

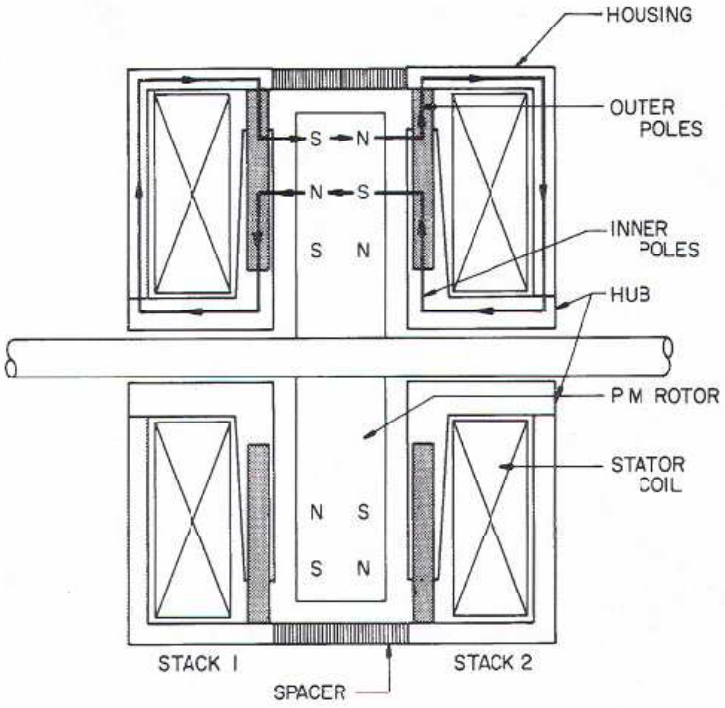

Figure 4. Cross-sectional view of the disk-rotor motor.

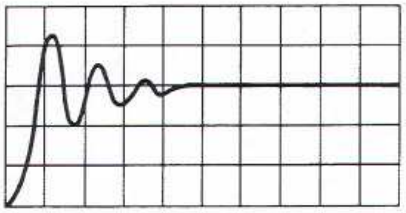

Figure 5. Single-step response.
One-phase-on excitation.
Horizontal: 10 msec/div.
Vertical: 1.25 deg/div.
30 Volts at 1.75 Amps.
8-ohm suppression.

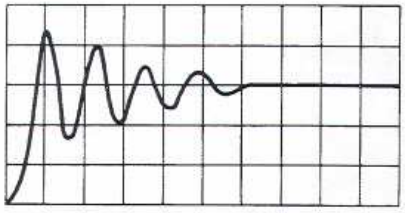

Figure 6. Single-step response.
Two-phase-on excitation.
Horizontal: 10 msec/div.
Vertical: 1.25 deg/div.
30 Volts at 1.75 Amps/phase.
8-ohm suppression.

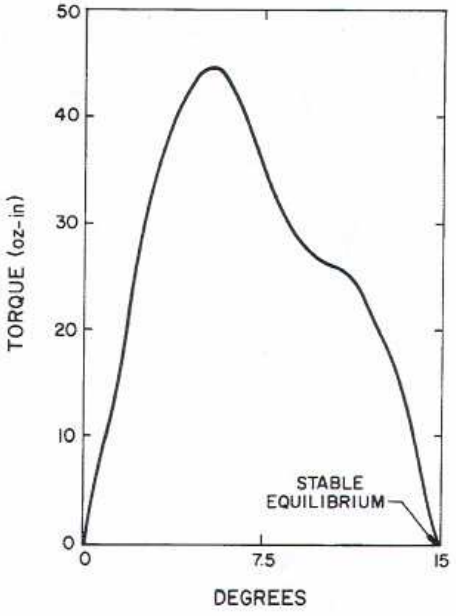

Figure 7. Static holding torque - one-phase-on.

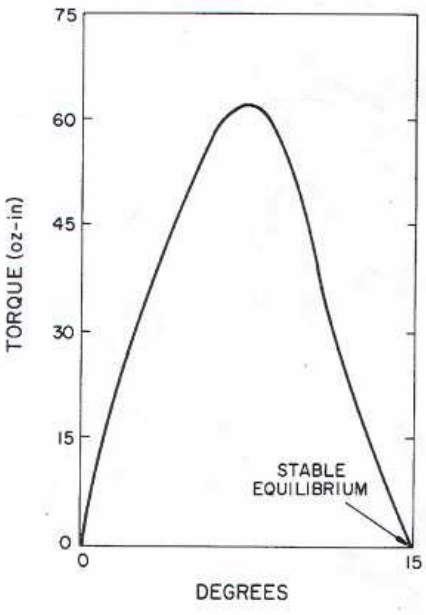

Figure 8. Static holding torque - two-phase-on.

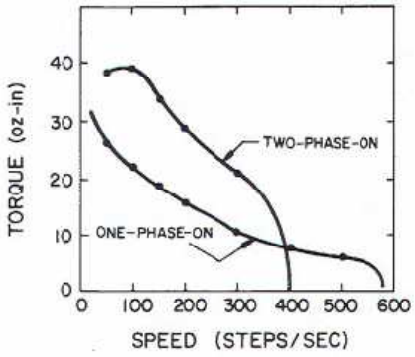

Figure 9. Torque-speed curves.

Ultimag® Size 4EM

Part Number: 199172-0XX

All catalogue products manufactured after April 1, 2004 are RoHS Compliant

Specifications

Dielectric Strength	1000 VRMS (23 awg); 1200 VRMS (24-33 awg)
Recommended Minimum Heat Sink	Maximum watts dissipated by the Ultimag are based on an unrestricted flow of air at 20°C, with the Ultimag mounted on the equivalent of an aluminium plate measuring 15.9 cm square x 0.32 cm thick
Thermal Resistance	7.6°C/watt with heatsink; 15.0°C/watt without heatsink
Rotor Inertia	8.43×10^{-7} (kgm²)
Peak Torque Rating (Tp)	0.32 Nm
Power Input	145 watts (stalled at Tp; 25°C; Pp)
Number of Phases	1
Static Friction (Tf)	7 mNm
-3dB Closed Loop	78 Hz
Maximum Winding	180°C
Number of Poles	6
Weight:	215 gms
Dimensions:	Ø41.66 mm x 26.3 mm L (See page B10)

Performance

Maximum Duty Cycle	100%	50%	25%	10%
K_M (mNm/√watt)	40.6	35.7	32.2	30.1
Maximum ON Time (sec) when pulsed continuously[2]	∞	40	15	4
Maximum ON Time (sec) for single pulse[2]	∞	108	34	9
Typical Energise Time (msec)[3]	6	5	4.5	3.5
Watts (@ 20°C)	14.5	29	58	145
Ampere Turns (@ 20°C)	510	721	1020	1613

Coil Data

awg (000)[4]	Resistance (@20°C)	# Turns[5]	VDC (Nom)	VDC (Nom)	VDC (Nom)	VDC (Nom)
23	0.71	104	3.2	4.5	6.4	10.1
24	1.54	174	4.7	6.7	9.4	14.9
25	2.15	195	5.6	7.9	11.2	17.6
26	3.01	219	6.6	9.3	13.2	20.9
27	5.70	320	9.2	12.9	18.3	28.9
28	8.09	368	10.8	15.3	21.7	34.3
29	14.40	515	14.5	20.4	28.9	45.7
30	20.11	575	18.9	24.2	37.7	59.6
31	34.40	774	22.3	31.6	44.6	71.0
32	56.60	1008	28.7	40.5	57.0	91.0
33	91.40	1288	36.0	51.5	73.0	115.0

How to Order

Add the coil awg number (0XX) to the part number (for example: to order a 25% duty cycle rated at 18.3 VDC, specify 199172-027).

Please see www.ledex.com (click on Stock Products tab) for our list of stock products available through our distributors.

[1] Continuously pulsed at stated watts and duty cycle

[2] Single pulse at stated watts (with coil at ambient room temperature 20°C)

[3] Typical energise time based on no load condition. Times shown are for half of full rotary stroke starting at centre-off position.

[4] Other coil awg sizes available — please consult factory

[5] Reference number of turns

WARNING: Exposed Magnet may affect pacemakers. In the event a product unit's magnet is exposed due to product disassembly, Pacemaker Wearers should distance themselves 3 metres from exposed magnet.

All specifications subject to change without notice.

References

Society., Incremental. 1981. Incremental Motion Control Systems and Devices: Proceedings, Tenth Annual Symposium, June 1981. Champaign, Ill. Incremental Motion Control Systems Society.

Motor Engineering. Chatsworth: NMB Technologies Corporation. Accessed December 1 2007, from: <nmbtc.com>.

Condit, Reston. 2004. "Stepping Motor Fundamentals." [Available Online] [Cited December 1, 2007] Available from www.microchip.com.

Solenoid Basic. Vandalia. Accessed December 1 2007, from: <www.ledex.com>.

Lazic, Anita, Browning, Bert, Nwabude, Tiffany, and Fallen, Tio. 2006. Axial Flux Permanent Magnet Micromotor Based on MEMS Technology. Thesis, Engineering, Florida State University, Tallahassee.